AFML-TR-69-117
Part V

EXPERIMENTAL PHASE EQUILIBRIA OF SELECTED BINARY, TERNARY, AND HIGHER ORDER SYSTEMS

Part V. The Phase Diagram W-B-C

E. RUDY

FOREWORD

The research described in this report was carried out under USAF Contract F 33 615-67-C-1513 by the Materials Research Laboratory, Aerojet-General Corporation, Sacramento, California. The contract was initiated under Project No. 7350, "Refractory Inorganic Nonmetallic Materials", Task No. 735001, "Refractory Inorganic Nonmetallic Materials: Nongraphitic", and was administered under the direction of the Air Force Materials Laboratory, Wright-Patterson Air Force Base, Ohio, with Captain P. J. Marchiando (MAMC) as Project Engineer. Dr. E. Rudy (now at the Oregon Graduate Center, Portland, Oregon) was the Principal Investigator.

This report covers work conducted during the period April 1967 through May 1969. It was submitted by the author February 1970.

Other reports issued, or in preparation, under USAF Contract AF 33 615-67-C-1513, are:

Part I.	The Phase Diagrams of the Systems Ti-Nb-C, Ti-Ta-C, and Ti-Mo-C.
Part II.	Effect of Re and Al Additions on the Metal-Rich Phase Equilibria in the Ti-Mo-C and Ti-Nb-C Systems
Part III.	Phase Studies in the V-Ta-C and Nb-Ta-C Systems
Part IV.	Effect of Mo and W Additions on the Subcarbide Solid Solutions in the V-Ta-C and Nb-Ta-C Systems.

The technical report has been reviewed and is approved.

W. G. RAMKE
Chief, Ceramics and Graphite Branch
Metals and Ceramics Division
Air Force Materials Laboratory

ABSTRACT

The ternary alloy system W-B-C was investigated experimentally by means of X-ray, melting point, DTA, and metallographic techniques on hot-pressed and heat-treated, as well as melted specimens, and a phase diagram from 1500°C through the melting range established.

No ternary phases are formed in the system and the mutual solubilities between carbide and boride phases are small. The solid-state sections (<2000°C) are characterized by two-phase equilibria existing between the phase pairs $W_2B + W_2C$, $W_2B + WC$, $WC + WB$, $WB + C$, $W_2B_5 + C$, $W_2B_5 + B_4C$, and $WB_{\sim 4} + B_4C$. The two-phase equilibrium $W_2B + WC$ is replaced by an equilibrium $W_2C + WB$ above 2150°C.

Fifteen ternary isothermal reactions have been found. Five are associated with pseudobinary eutectic equilibria, six with ternary eutectics, and the remaining four with class II ternary four-phase reaction isotherms.

TABLE OF CONTENTS

LIST OF ILLUSTRATIONS

LIST OF ILLUSTRATIONS (Cont'd)

LIST OF ILLUSTRATIONS (Cont'd)

I. INTRODUCTION AND SUMMARY

A. INTRODUCTION

Next to the refractory carbides, the borides of the refractory transition metals are among the highest melting materials known. While they compare in hardness and mechanical properties with the carbides, the borides generally have much better oxidation resistance at elevated temperatures. In spite of these interesting properties, however, efforts undertaken to utilize the borides in parts for high temperature service are hampered by their extreme brittleness and their reactivity with other alloys; the latter property especially has so far prevented the successful development of suitable metal binder alloys to reduce the mechanical and thermal shock sensitivity of the compounds.

To gain a better understanding of the behavior of refractory boride and carbide phases in the presence of other high melting compounds, including other borides and carbides, as well as silicides, nitrides, and metal phases, a systematic study of ternary alloy systems was initiated a few years ago.[1] These investigations have led, especially in the case of the carbides, to a comprehensive interpretation and classification of the high temperature reaction behavior of these compounds.

The current effort was undertaken to study the high temperature phase equilibrium characteristics of a Me-B-C system involving a group VI refractory transition metal, after borocarbide systems involving group IV metals (Ti,Zr,Hf) have been treated under the preceding program.[1] Points of specific interest included phase equilibria involving boron carbide, the mutual solubilities of carbide and boride phases, and the eventual formation of new ternary phases.

B. SUMMARY

The ternary alloy system W-B-C was investigated experimentally by means of X-ray, melting point, metallographic, and differential-thermoanalytical techniques, using hot-pressed, and sintered, as well as melted specimens, and a phase diagram was established. An isometric view of the system is shown in Figure 1.

Fifteen ternary isothermal reactions occur in the experimentally investigated temperature range from 1500° C through melting (Figure 2). Five isothermal reactions are associated with the formation of pseudobinary eutectic equilibria between the phase pairs $W_2B + W_2C$ (2370° C, 41 mole% W_2C), $WB + W_2C$ (2330° C, 38 mole% W_2C), $WB + C$ (2360° C, 13 At.% C), $W_2B_5 + C$ (2275° C, 7 At.% C), and $W_2B_5 + B_4C$ (2220° C, 24 mole% B_4C). Six reaction isotherms are associated with ternary eutectics,

$$L \rightleftarrows W + W_2C + W_2B \text{ at } 2355^\circ C$$

$$L \rightleftarrows W_2C + W_2B + WB \text{ at } 2305^\circ C$$

$$L \rightleftarrows W_2C + WC + WB \text{ at } 2300^\circ C$$

$$L \rightleftarrows WB + W_2B_5 + C \text{ at } 2240^\circ C$$

$$L \rightleftarrows W_2B_5 + C + B_4C \text{ at } 2180^\circ C$$

$$L \rightleftarrows WB_{\sim 4} + B + B_4C \text{ at } 1950^\circ C,$$

and four with class II (two-over-two) four-phase equilibria:

$$L + \alpha\text{-}WC_{1-x} \rightleftarrows W_2C + WC \text{ at } 2570^\circ C$$

$$L + C \rightleftarrows WC + WB \text{ at } 2350^\circ C$$

$$W_2C + WB \rightleftarrows W_2B + WC \text{ at } 2150^\circ C$$

$$L + W_2B_5 \rightleftarrows WB_{\sim 4} + B_4C \text{ at } 2000^\circ C$$

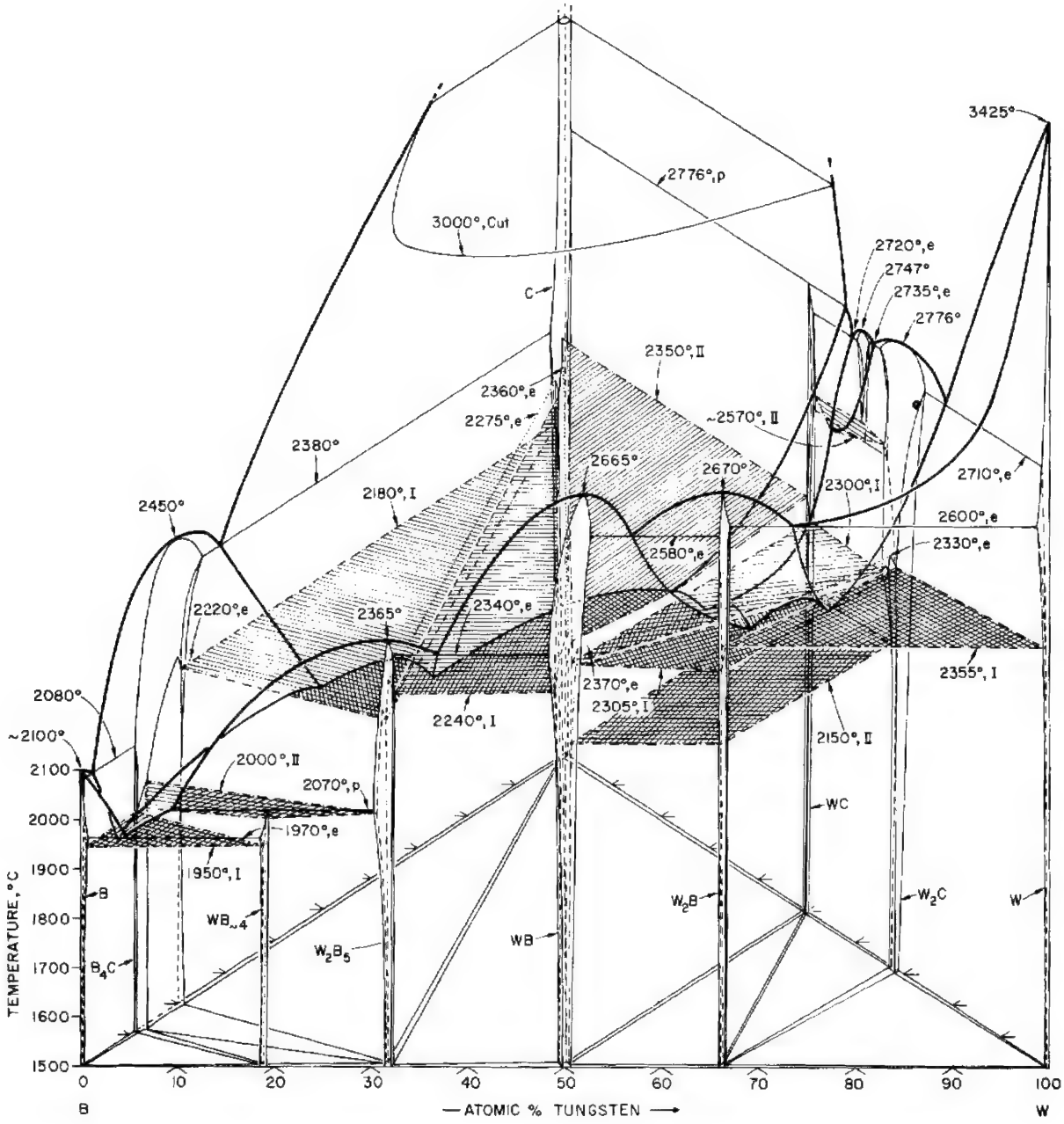

Figure 1. Isometric View of the Constitution Diagram W-B-C.

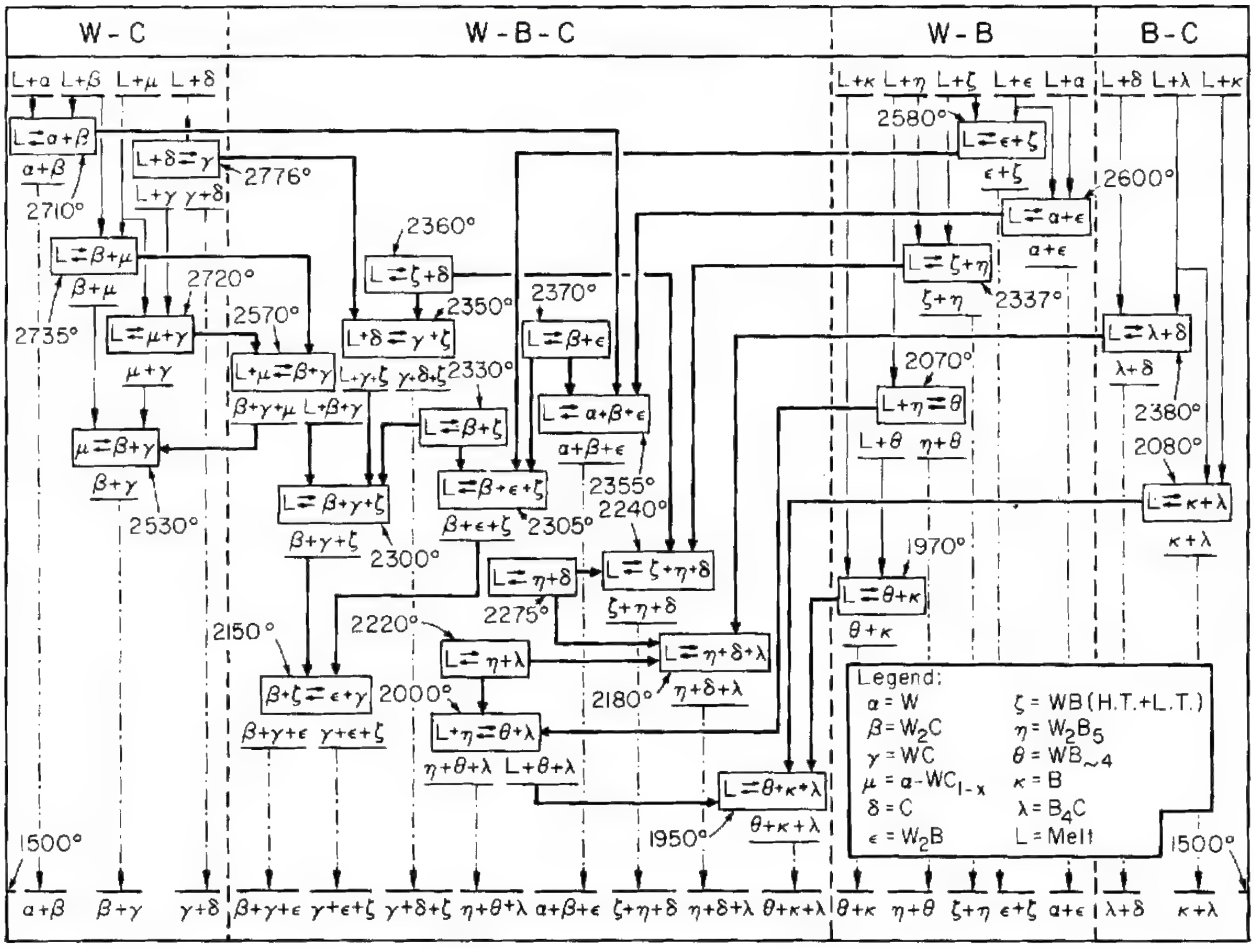

Figure 2. Reaction Diagram for the W-B-C System

A projection of the melting troughs and liquidus isotherms in the system is depicted in Figure 3. Additional isothermal reactions resulting from the high temperature transformation of the binary WB and the sublattice order-disorder transitions in W_2C were not studied in detail and thus were not included in the phase diagram assemblies.

The lower temperature (<2100° C) solid state-sections in the system are characterized by very limited mutual solubilities between boride and carbide phases and the existence of two-phase equilibria between the pairs

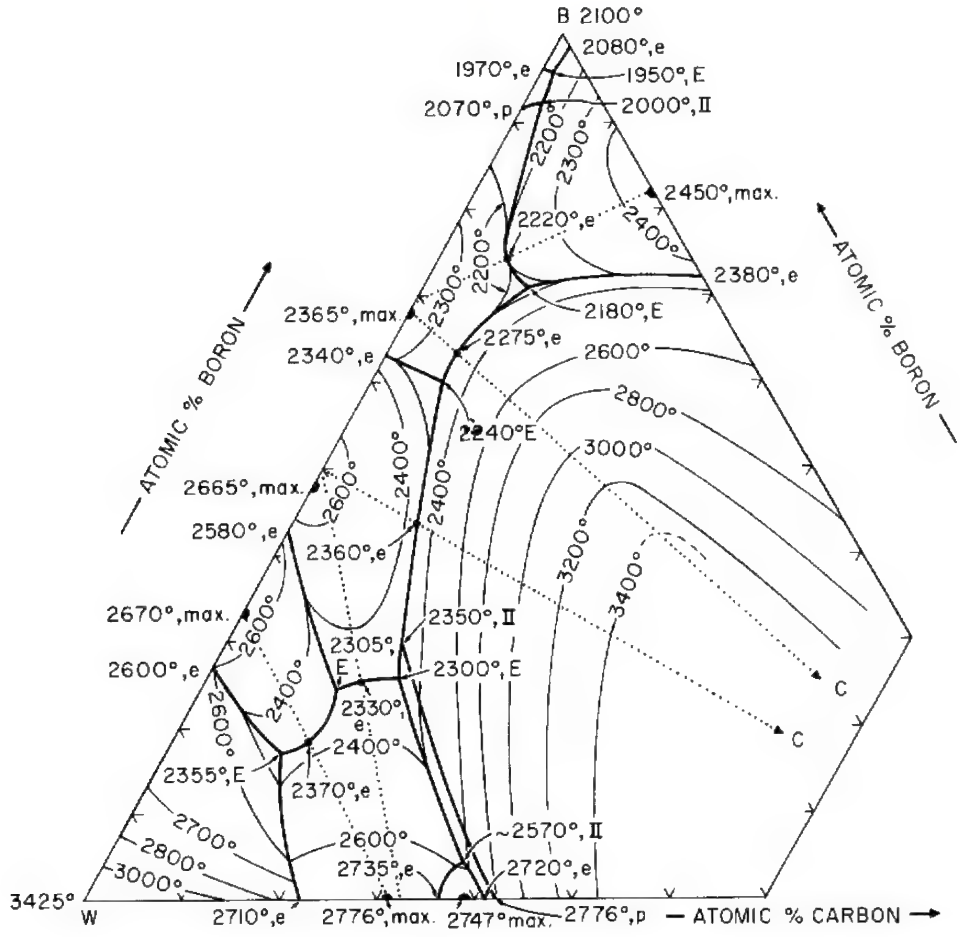

Figure 3. Liquidus Projections in the W-B-C System

$W_2B + W_2C$, $W_2B + WC$, $WC + WB$, $WB + C$, $W_2B_5 + C$, $W_2B_5 + B_4C$, and $WB_{\sim 4} + B_4C$. Above 2150° C, the equilibrium $W_2B + WC$ is replaced by an equilibrium between WB and W_2C.

II. LITERATURE REVIEW

The most recent version of the phase diagram of the W-C system, compiled from previous work[2,3,4] as well as our investigations[5,6], is shown in Figure 4. The system contains three intermediate phases of which two, W_2C and $\alpha\text{-}WC_{1-x}$(B1), melt congruently, while the third, WC, decomposes

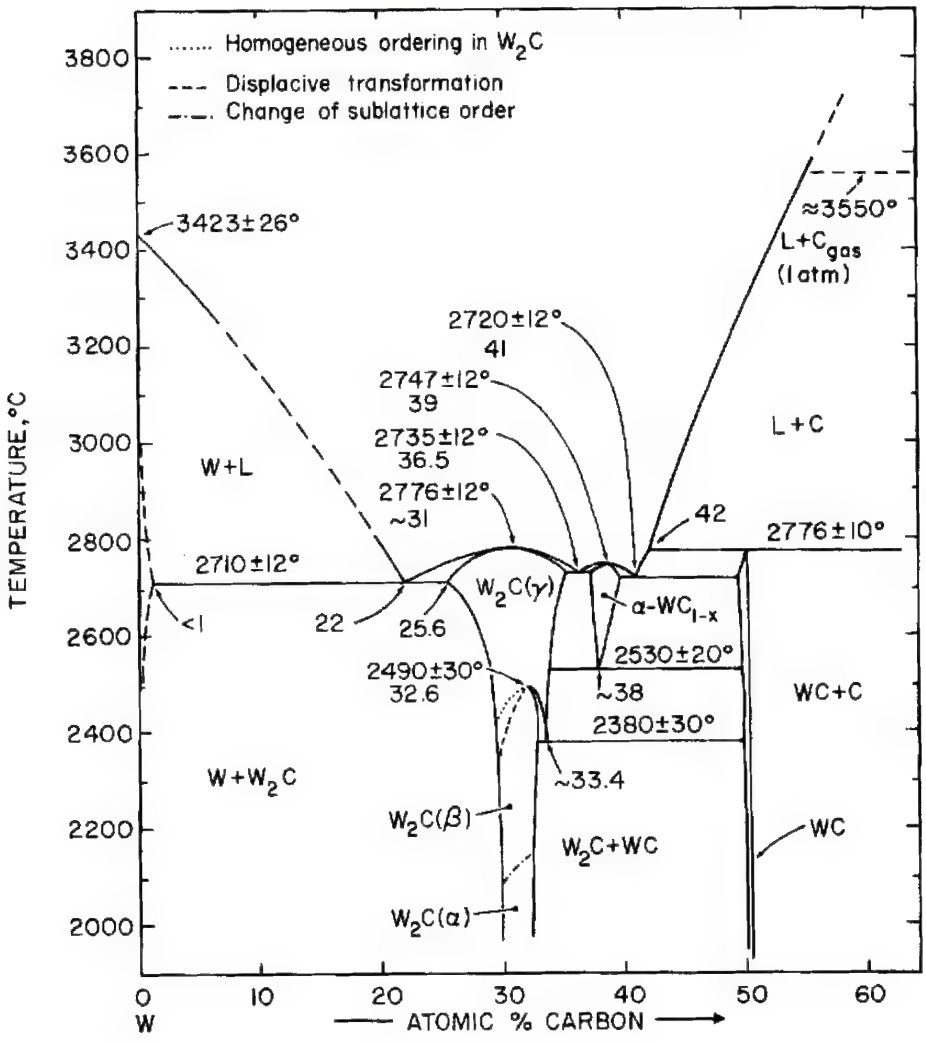

Figure 4. Constitution Diagram Tungsten-Carbon

in a peritectic reaction at 2776° C. The subcarbide, W_2C, exists in several states of sublattice order (Table 1) and shows a complex transition behavior (Figure 4). The cubic carbide α-WC_{1-x} is stable at high temperatures only and decomposes in a rapid eutectoid reaction at 2530° C into the disordered modification of W_2C and tungsten monocarbide.

Although the structure of the tungsten boride phases have been established for quite some time[11,13], the phase diagram of the tungsten-boron

Table 1. Structure and Lattice Parameters of Phases in the Tungsten-Carbon and Tungsten-Boron System

Phase	Structure	Lattice Parameters, Å
W_2C	hex., L'3-type(>2480° C)(7)	a=2.985 c=4.716 at 29.5 At.% C
	hex., C6-type (8)	a=3.000 c=4.730 at 32.8 At.% C (5)
	Orthorh. ζ-Fe_2N-type (2100 to 2480 °C)	a=4.738 b=6.009 at 32.6 At.% C (7) c=5.193
	hex., ϵ-Fe_2N-type	a=5.184 c=4.721 (9)
α-WC_{1-x}	fcc., B1-type	a=4.215 (2,3) a=4.220 at ~38 At.% C (5)
WC	hex., B_h-type (D^1_{3h}-P6m 2)	a=2.9062 a=2.8368 (10)
W_2B	Tetr., C16-type	a=5.564; c=4.740 (11) a=5.570 to 5.572 c=4.744 to 4.746 (12)
WB Low Temp. Modif.	Tetrag., Bg-type	a=3.115; c=16.93 (11) a=3.093 to 3.120 c=16.99 (12)
WB High Temp. Modif.	Orthorh., CrB-type	a=3.19; b=8.40; c=3.07 (13) a=3.142; b=8.506; c=3.065 (12)
W_2B_5	hex., $D8_h$-type	a=2.982; c=13.87 (11) a=2.980; c=13.88 (12)
WB_n (n~4)	hex., $P6_3/mmC$	a=5.200; c=6.340 (14) a=3.004; c=3.174 (hex. subcell)(15)

system was established only recently by E. Rudy et al. (Figure 5)[12]. The system contains four phases, W_2B, WB, W_2B_5, and $WB_{\sim 4}$ (Table 1), of which the first three melt congruently, whereas the boron-richest phase was indicated[12] to melt under decomposition. The monoboride exists in a tetragonal modification below approxima tely 2100° C, and an orthorhombic high temperature polymorph, which is stable between ~2100° C and the melting point.

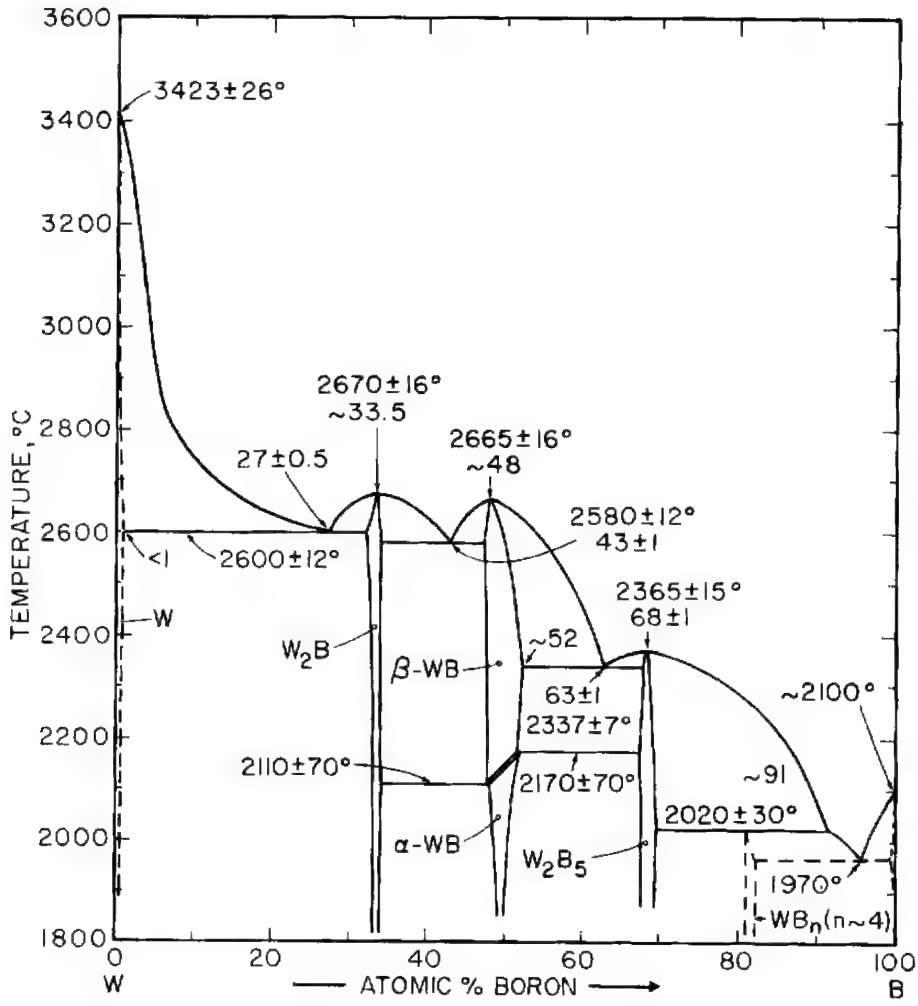

Figure 5. Constitution Diagram Tungsten-Boron

The boron carbon system[16] (Figure 6) contains one intermediate phase, B_4C, which has an extended range of homogeneity. The structure of B_4C is rhombohedral, with a_R=5.19Å, $\alpha = 66°18'$[17].

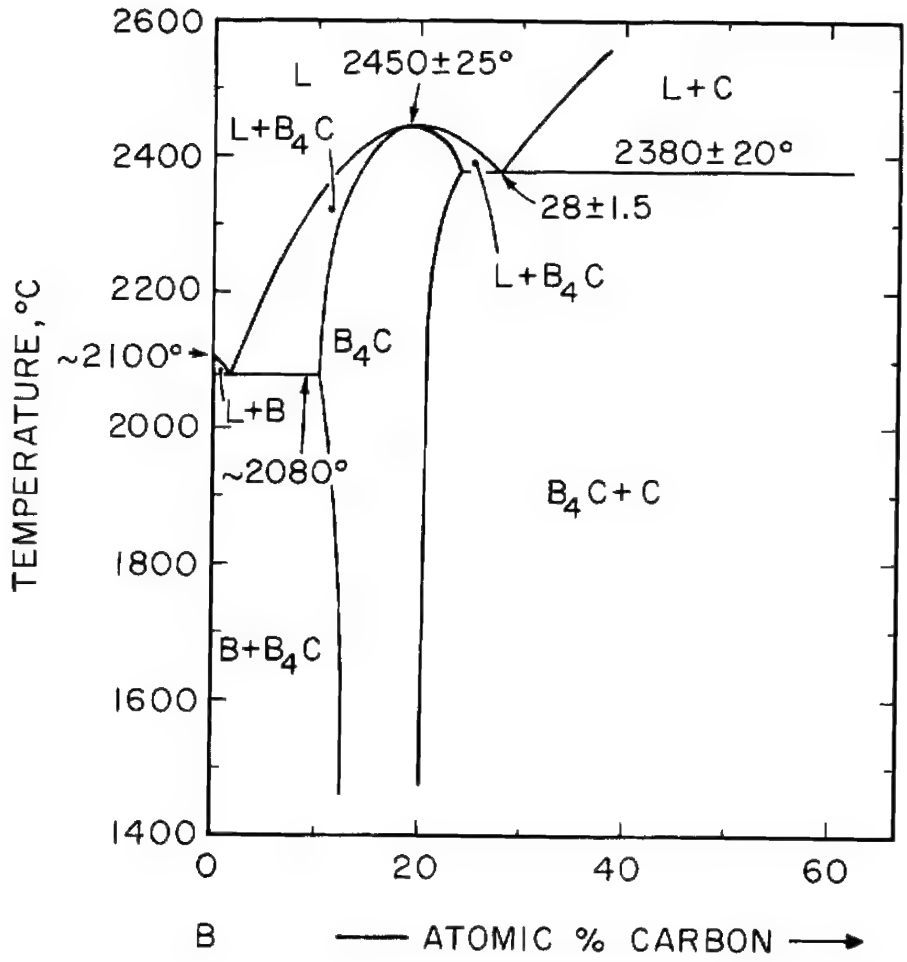

Figure 6. Constitution Diagram Boron-Carbon.
(Compiled from R.T. Doloff [18], R.P. Elliott[19], and Own Investigations)

An isothermal section of the W-B-C system at 1700°C was established by E. Rudy et al.[15] (Figure 7). Qualitative investigations of the behavior of borides in the presence of carbon have been carried out by Glaser[20] and Brewer and Haraldsen[21].

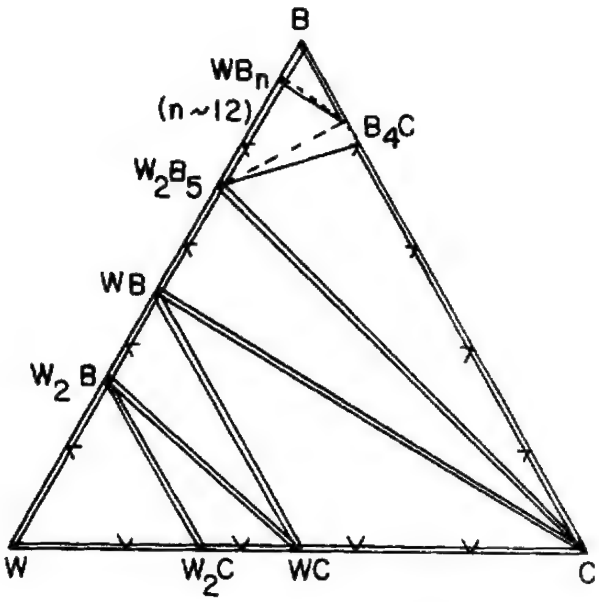

Figure 7. Section of the W-B-C System at 1700° C. (After E. Rudy et al., 1963).

III. EXPERIMENTAL

A. STARTING MATERIAL AND ALLOY PREPARATION

The elemental powders, as well as master alloys of W_2B_5 and WC, served as the starting materials for the preparation of the experimental alloys.

The tungsten powder (Wah Chang Corp., Albany, Oregon) contained the following impurities (in ppm): Mo-50, O-720, Fe-40; Ni-20; N-430, and the sum of other metallic contaminants-<60. The average grain size of the tungsten powder was 6.8 microns, and a lattice parameter of 3.1665Å was determined from a Debye-Scherrer exposure with Cu-K_α radiation.

The analysis of the spectrographic grade graphite powder (National Carbon Corp.) was as follows (in ppm): Al-0.3; Cu-0.1; Fe-0.2; Mg-0.1; and Si-0.2.

Boron powder of 99.55% overall purity was purchased from United Mineral and Chemical Corporation, New York. Major impurities were iron (0.25%), and carbon (0.1%).

Tungsten monocarbide was prepared by reacting the cold-compacted mixtures of the elemental powders in a graphite-element furnace for 4 hours at 2100° C under hydrogen. After cooling under vacuum, the reaction lumps were comminuted to a grain size less than 60 microns in carbide-lined ball mills. Cobalt traces picked up during milling were removed by acid-leaching in a mixture of hydrochloric and sulfuric acid, the resulting slurry centrifuged, washed with ether, and then vacuum dried. Chemical analysis indicated a total carbon content of 50.7 ± 0.3 At.%, and an oxygen contamination level of less than 150 ppm. The lattice parameters measured were a = 2.906Å, and c = 2.837Å.

W_2B_5 was prepared by direct combination of the elements at high temperatures. The well-blended mixture of tungsten and boron powder was cold compacted, the compacts stacked into tantalum cans, and the assembly loaded into the heating zone of a graphite element high temperature furnace. The reaction was initiated at about 1200° C and brought to completion by a two hour vacuum treatment at 1750° C. The reaction lumps were then crushed, acid leached, and further processed in the same manner as described for the tungsten monocarbide. Chemical analysis determined a boron content of 70.7 ± 0.5 At.%, and a carbon content of 0.12 Wt.%. The following impurities were determined spectrographically: Fe-500, Si-100, Mg-100, Al-500, Ca-100, Cu-100, Ni-100, Mn-100, Cr-100, Mo-100, Ti-600. The

lattice parameters measured from an exposure with Cu-K_α radiation, were a=2.982Å, and c=13.88Å.

Specimens for the experimental investigations were prepared by short duration hot pressing of the ingredient mixtures in graphite dies at temperatures between 1800 and 2200° C. Specimens for melting point and DTA-studies were used in the as-pressed conditions and were equilibrated in the melting point or DTA-furnace prior to the runs. The heat treatment schedules for the alloys prepared for the determination of the isothermal sections of the system were 140 hrs at 1500° C, and 6 hrs at 2000° C. To establish the temperature change of certain equilibria in the solidus region and also to obtain rapid cooling rates, selected alloys were equilibrated in the melting point furnace and tin-quenched. Mostly for metallographic purposes, a piece of each alloy was also arc melted under helium in a non-consumable electrode arc furnace.

B. DETERMINATION OF MELTING TEMPERATURES AND DIFFERENTIAL THERMAL ANALYSIS

Melting temperatures of the alloys were determined with the Pirani-technique, using a high purity helium atmosphere of 1 atm pressure. The design of the apparatus used in this laboratory and temperature calibration procedures have been described in detail in earlier publications[22, 23].

The DTA-runs[23] were also made under helium, using graphite as container material and tantalum monocarbide as comparison standard.

C. METALLOGRAPHIC, X-RAY, AND CHEMICAL ANALYSIS

For the microscopic inspections of the alloy structures, the samples were mounted in a mixture of diallylphtalate and lucite-coated copper powder. After coarse grinding on silicon carbide papers (grit sizes

between 120 and 600), the samples were polished on nylon cloth, using a suspension of 0.3 micron alumina in a 5% chromic acid solution. After polishing, the samples were electroetched in a 2% aqueous solution of sodium hydroxide.

Boron in the alloys was determined by dissolution of the powdered samples in a melt of pre-dried sodium carbonate at 1000° C. The resulting melt was dissolved in water, the excess carbonate removed by barium hydroxide, and the boric acid determined by differential titration of the boro-mannitol complex with N/10 NaOH between pH-values of 5.3 and 8.5. The consistence of the data obtained by this method varied between about ± 0.1 and ± 1 At.% B absolute.

Carbon was determined by the standard combustion technique, using a commercial Leco carbon analyzer. Oxygen, nitrogen, and hydrogen were analyzed by the gas-fusion technique, while low level metallic impurities were determined semiquantitatively by spectrographic methods.

X-ray powder diffraction patterns using Cu-K_α radiation were prepared from all alloys fabricated in the course of the system investigation.

IV. RESULTS

A. EXPERIMENTAL STUDIES

Due to the very limited mutual solubilities, the experimental investigation and the interpretation of the results was straight-forward and simple.

The X-ray evaluation of the alloy series equilibrated at 1500° C (Figure 8) substantially confirmed our previous findings concerning the gross

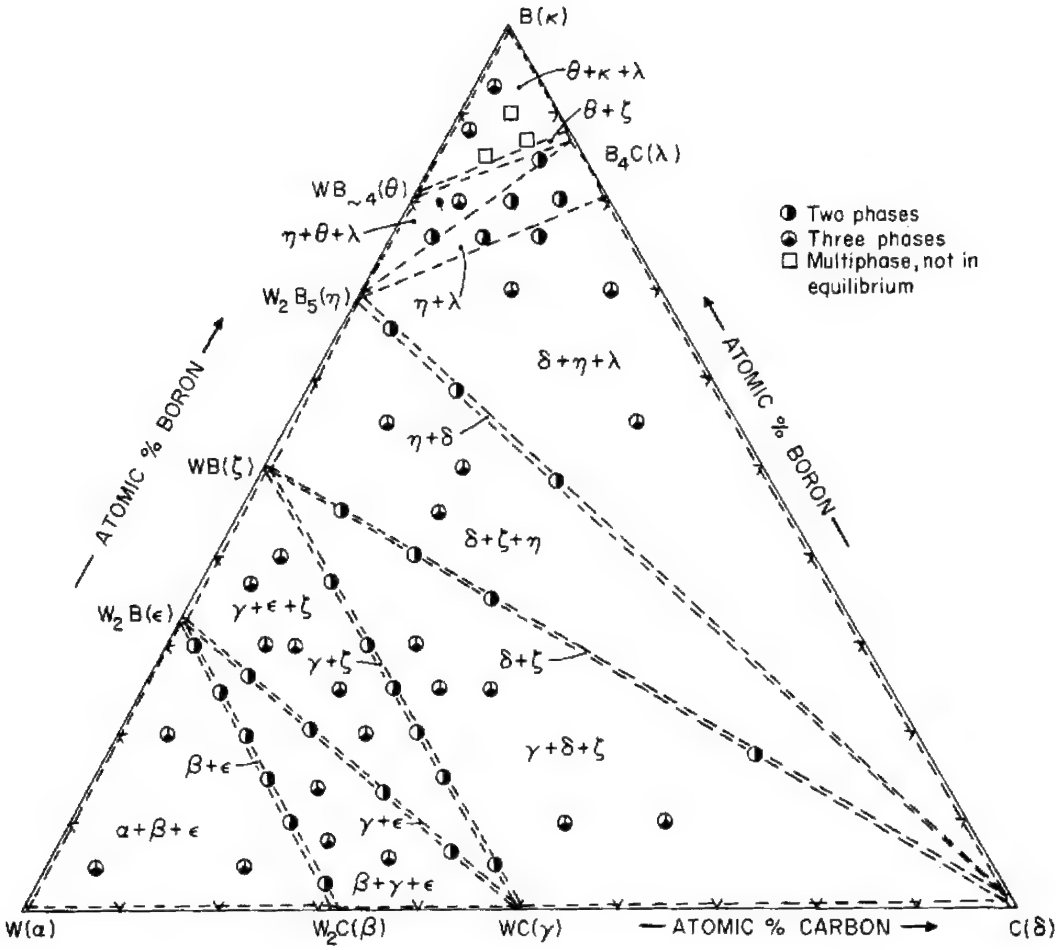

Figure 8. Qualitative (X-Ray) Phase Evaluation of the Alloy Series Heat-Treated at 1500° C.

features of the system below 2000° C[15]. Two-phase equilibria are formed between the phase pairs $W_2B + W_2C$, $W_2B + WC$, $WB + WC$, $WB + C$, $W_2B_5 + C$, $W_2B_5 + B_4C$, and $WB_{\sim 4} + B_4C$. The lattice parameters of the phases in the ternary alloys coincided within the error limits with those of the pure binary phases. The ternary homogeneity ranges of boride and carbide are therefore small, a result, which was independently corroborated by metallographic studies.

The phase equilibria at solidus temperatures (Figure 9) are very similar to those at lower temperatures. The only significant change involves a switch of the two-phase equilibrium $W_2B + WC$ to another equilibrium between W_2C and WB . DTA-studies of alloys located within the concentration range $W_2B + W_2C + WC + WB$ indicated a temperature of 2150°C for the nonvariant equilibrium

$$W_2B + WC \xrightarrow[T \geq 2150^\circ C]{} W_2C + WB$$

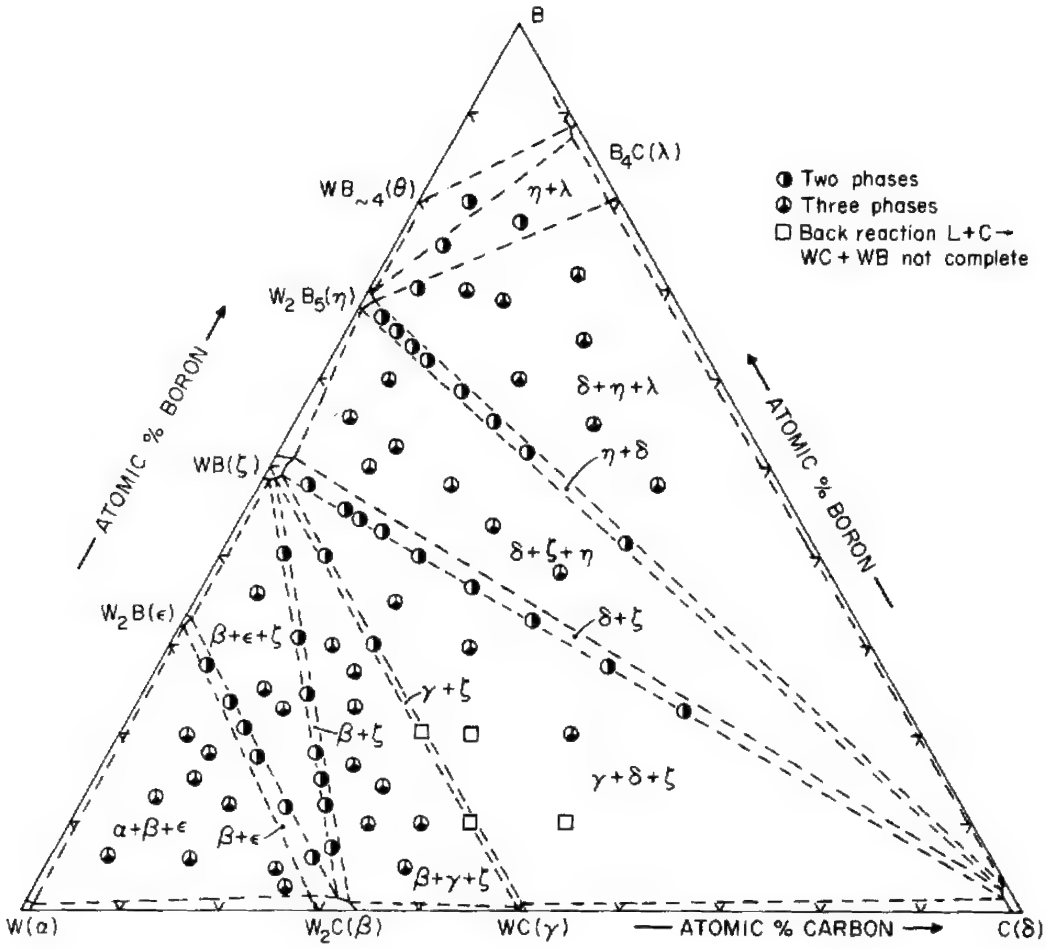

Figure 9. Qualitative (X-Ray) Phase Evaluation of As-Melted W-B-C Alloys.

This result was independently confirmed by X-ray analysis of alloys equilibrated at, and quenched from, temperatures above and below the four-phase plane. DTA-studies also ascertained that the transformation temperatures of WB are practically unaffected by the presence of carbon (Figures 10 and 11).

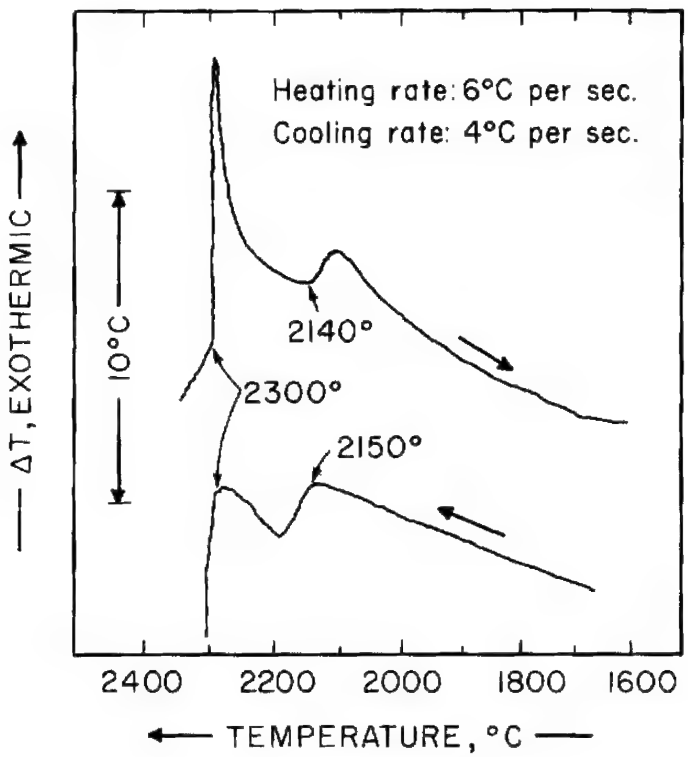

Figure 10. DTA-Thermograms Indicating a Solid-State Reaction Around 2150° C in an Alloy W-B-C (57-30-13 At.%).

After the gross features of the high temperature phase equilibria had been delineated by these preliminary studies, the subsequent effort concentrated on locating the nonvariant equilibria in the system by a combination of melting point, DTA, and metallographic techniques.

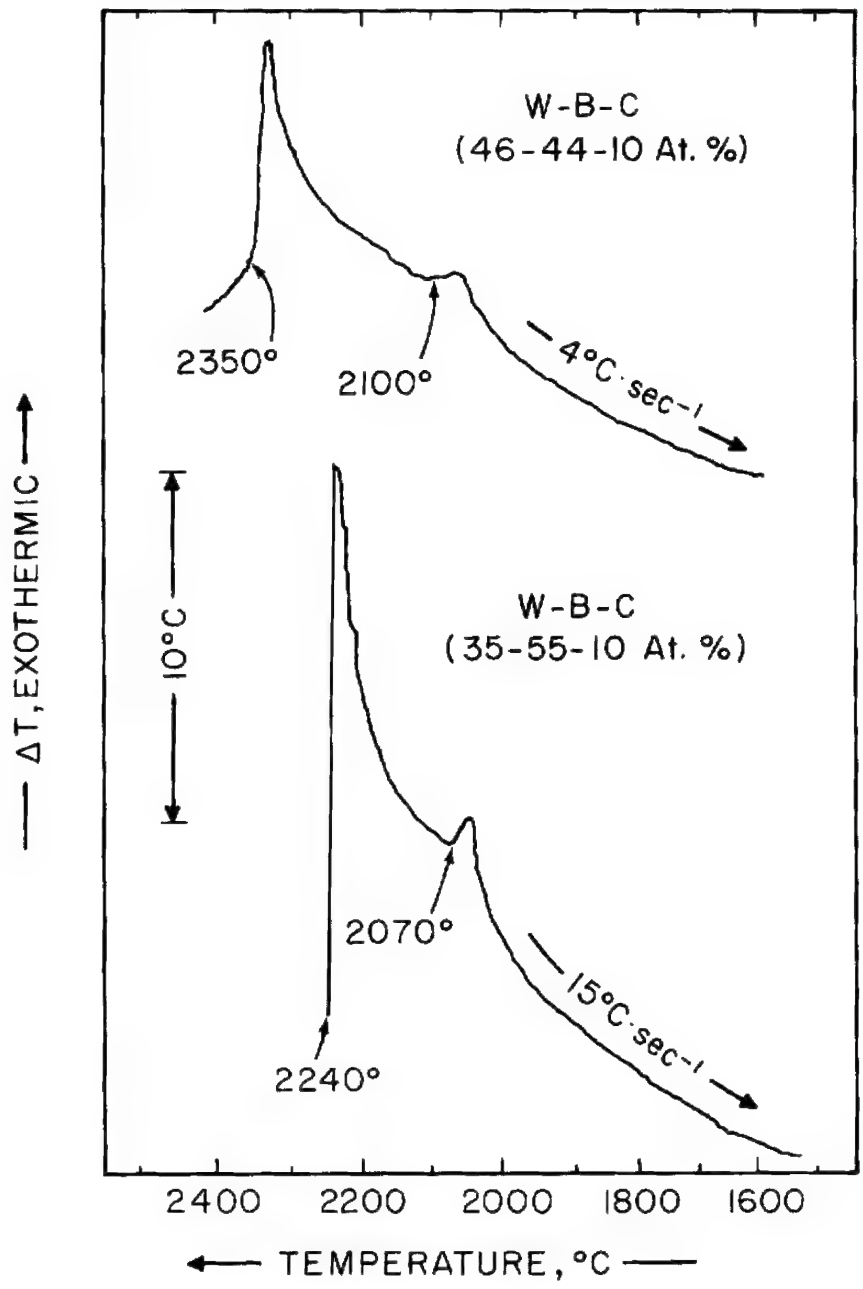

Figure 11. Transformation of the Orthorhombic High Temperature Modification of WB into the Tetragonal Low Temperature Form in Ternary W-B-C Alloys at ~2100°C.

Melting point measurements and microscopic inspection of the as-melted alloys established the existence of a pseudobinary eutectic equilibrium between W_2B and W_2C (Figures 12, 13, and 14). Because of the formation of eutectic equilibria between W and W_2C, and W and W_2B in the respective binaries and the absence of ternary compounds, only a ternary eutectic equilibrium is possible between the three phases $W + W_2C + W_2B$. Melting point as well as solidus points obtained by differential thermal analysis yielded a mean temperature of 2355° C for this ternary eutectic, and a eutectic composition of W-B-C (71-17-12 At.%) was derived by microscopic inspection of the alloys. Typical microstructures of melted alloys located in the vicinity of the ternary eutectic are shown in Figures 16, 17, and 18.

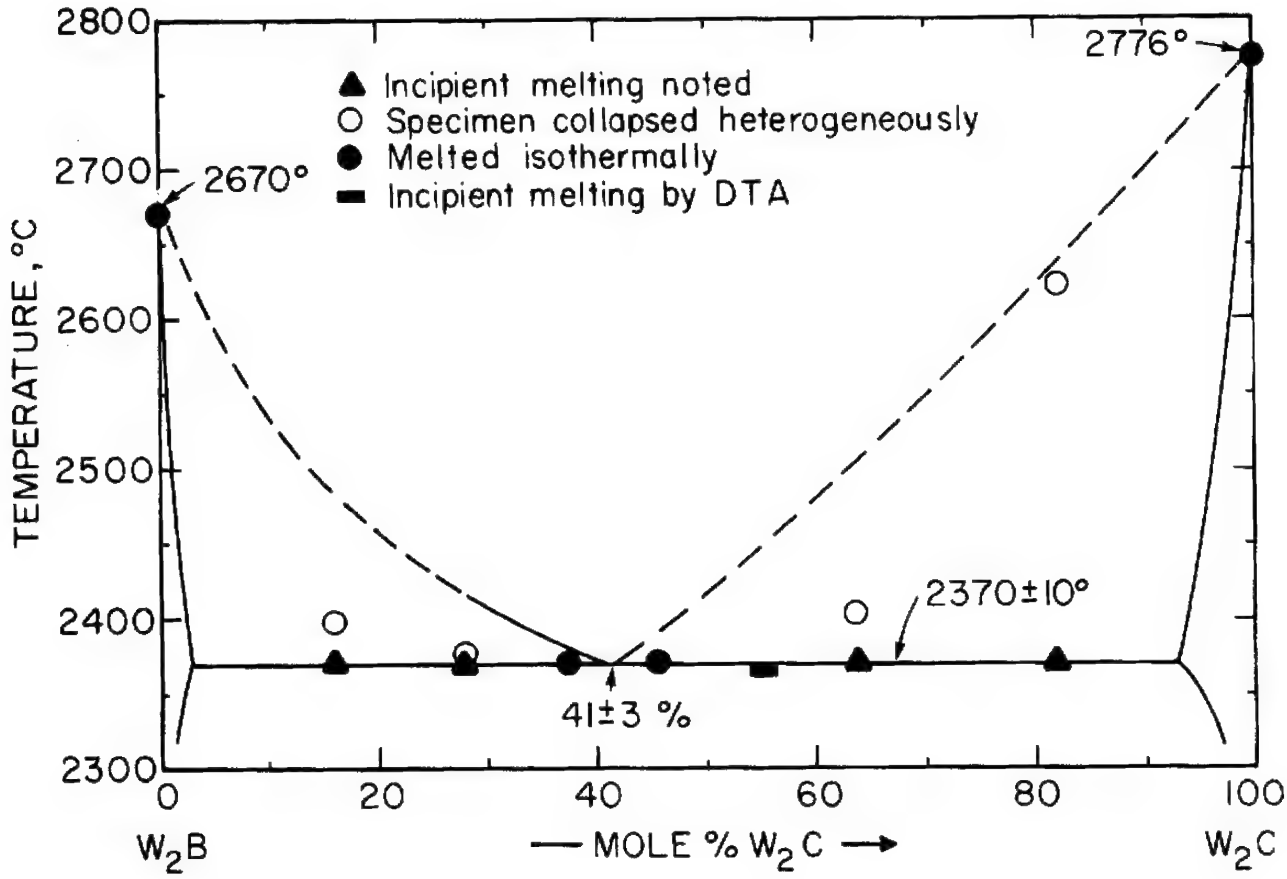

Figure 12. Melting Temperatures of Alloys Located at the Pseudobinary Eutectic Section W_2B-W_2C.

Figure 13. W-B-C (67-24-9 At.%), Melted and Rapidly Cooled. X440

Primary W_2B Crystals in a Matrix of W_2B + W_2C Eutectic.

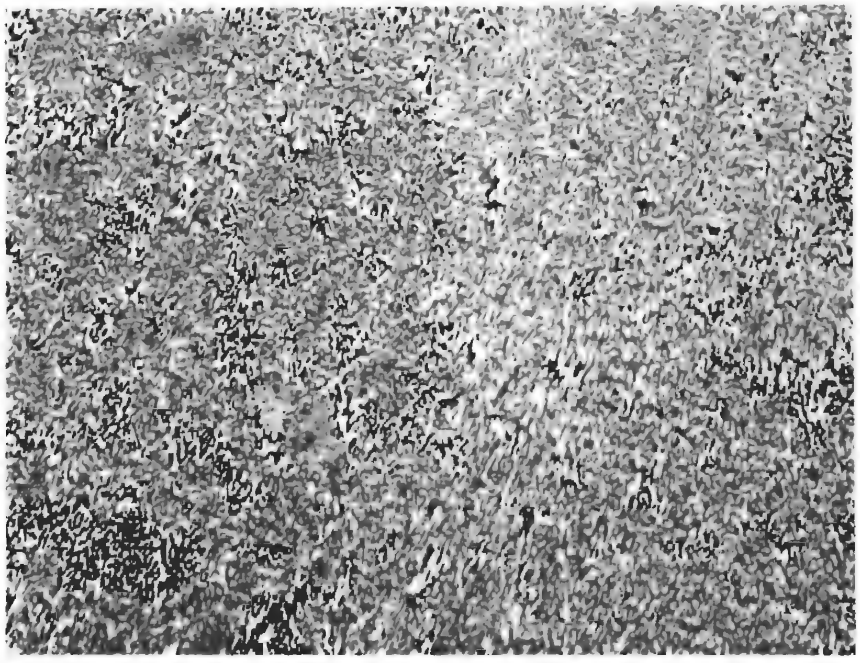

Figure 14. W-B-C (68-18-14 At.%), Melted and Rapidly Cooled. X680

W_2C + W_2B Pseudobinary Eutectic.

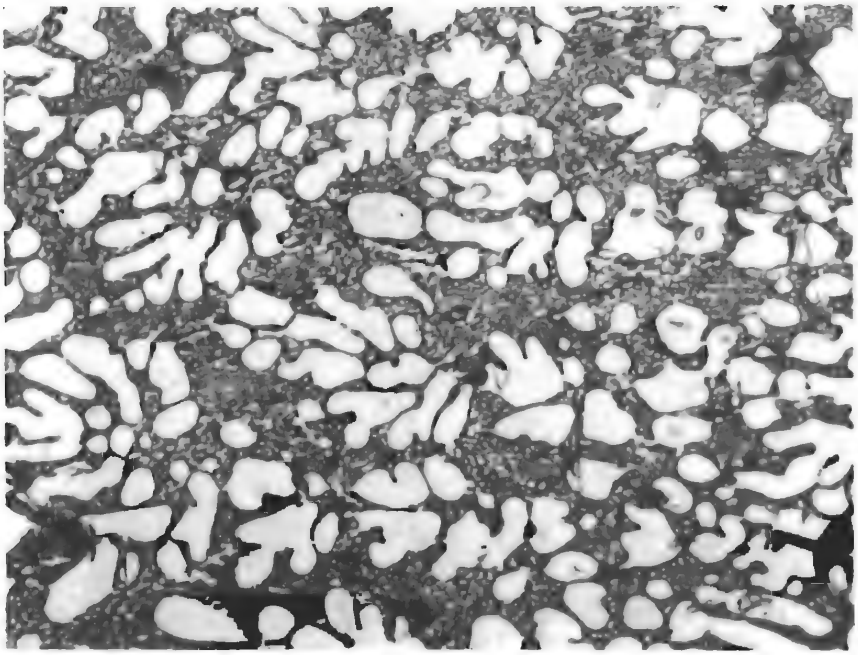

Figure 15. W-B-C (67-12-21 At.%), Rapidly Cooled from Liquidus Temperatures. X680

Primary W_2C in a Matrix of W_2B + W_2C Eutectic.

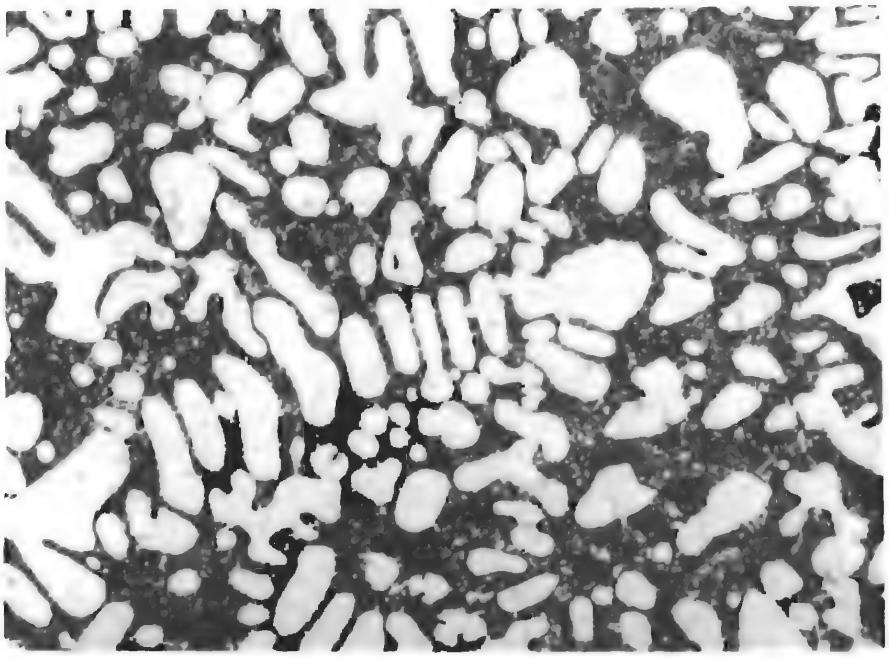

Figure 16. W-B-C (80-10-10 At.%), Melted and Rapidly Cooled. X720

Primary Tungsten (Rounded, Light Grains) in a Matrix of Ternary W + W_2C + W_2B Eutectic.

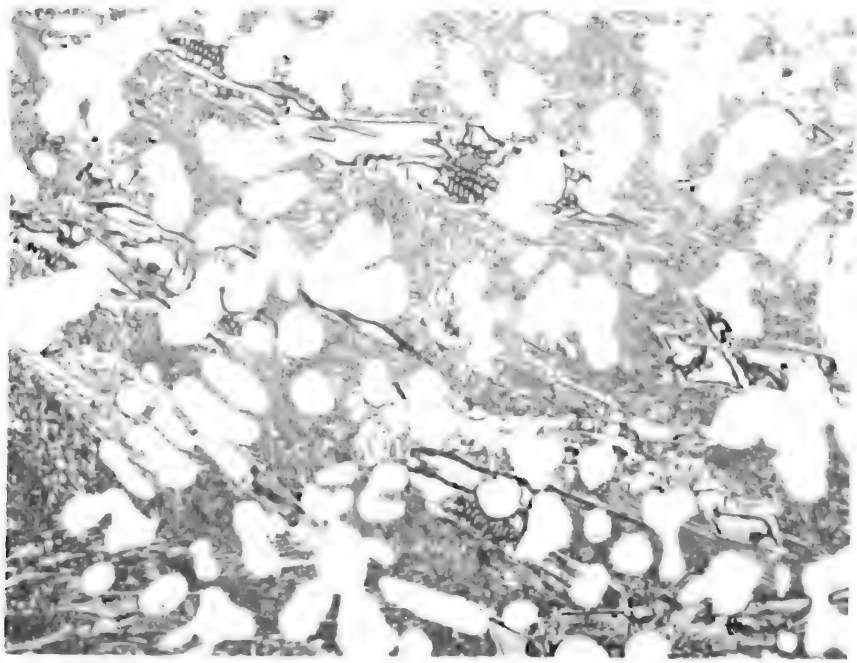

Figure 17. W-B-C (75-15-10 At.%), Melted and Rapidly Cooled. X440

Primary Tungsten, Smaller Amounts of Secondary W_2B, and Ternary $W + W_2B + W_2C$ Eutectic.

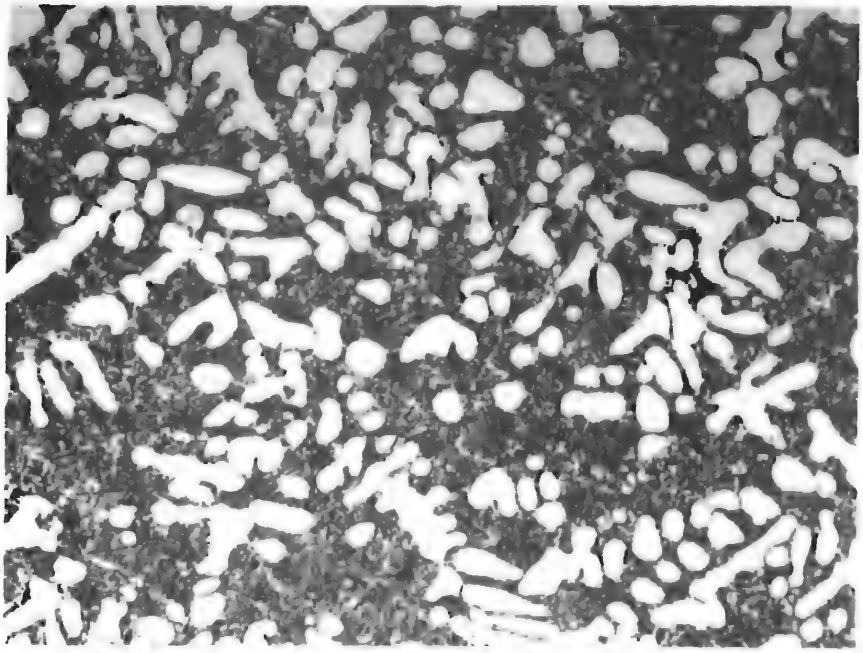

Figure 18. W-B-C (73-12-15 At.%), Melted and Rapidly Cooled. X680

Primary $W + W_2C$, Formed During Solidification Along the Eutectic Trough $W + W_2C$, in a Matrix of $W + W_2C + W_2B$ Eutectic.

The phase WB and W_2C also form a pseudobinary eutectic pair (Figures 18, 20, 21). The phase mixture W_2C + WB, which is stable only above 2150° C, is gradually converted to a mixture of WC + W_2B (Figures 22 and 23) upon reannealing of as-melted and quenched samples at temperatures below 2100° C.

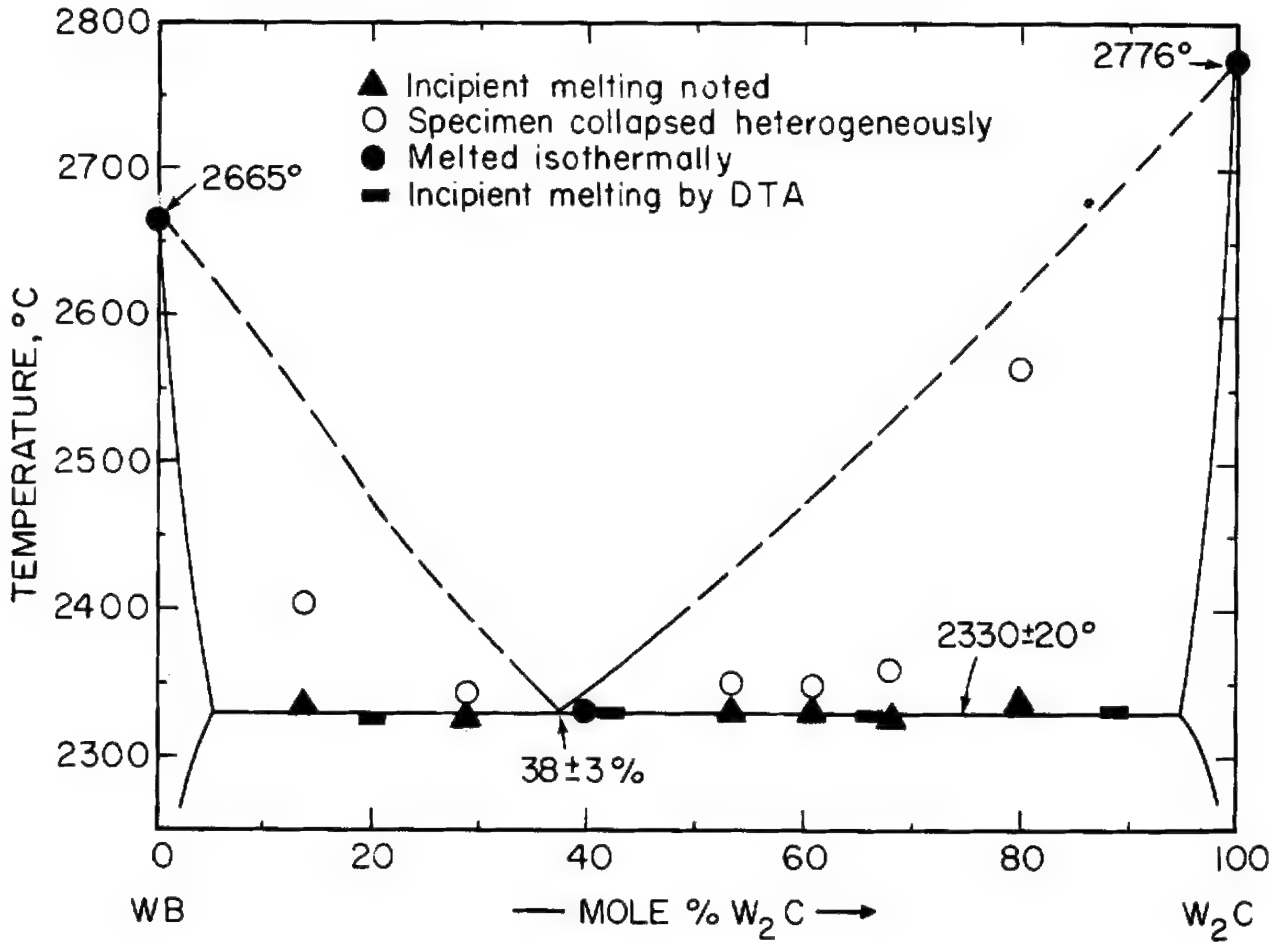

Figure 19. Melting in Alloys at the Pseudobinary Eutectic Section WB-W_2C.

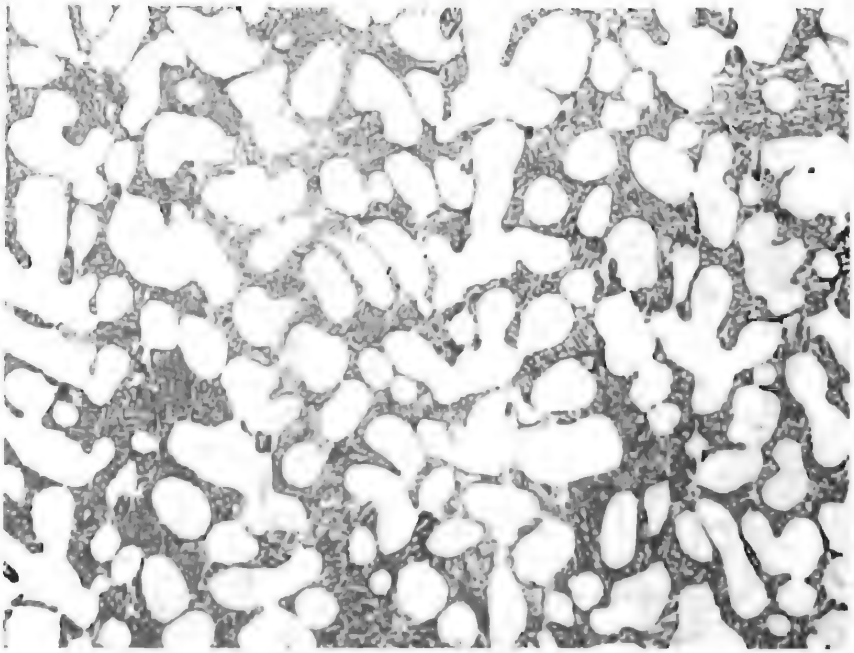

Figure 20. W-B-C (64-11-25 At.%), Rapidly Cooled from Liquidus Temperatures. X680

Primary W_2C in a Matrix of W_2C + WB Eutectic.

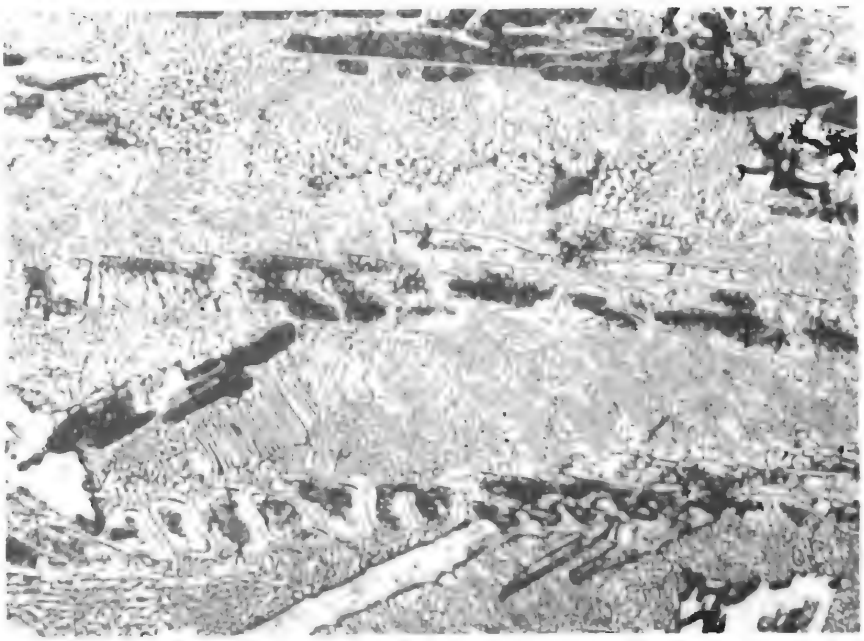

Figure 21. W-B-C (58-30-12 At.%), Rapidly Cooled from Liquidus Temperatures. X400

Primary WB (Showing Intragranular Transformation and Precipitation Structure) in a WB + W_2C Pseudo-binary Eutectic Matrix.

Figure 22. W-B-C (60-20-20 At.%), As-Melted X520

Primary W_2C in a W_2C + WB Pseudobinary Eutectic Matrix. X-Ray: W_2C + WB

Figure 23. Sample Shown in Figure 28 Reequilibrated for 3 hours at 1800°C and Rapidly Cooled. X520

X-Ray: WC + W_2B

A ternary eutectic between the phases W_2C, W_2B, and WB is located at 2305° C and a composition W-B-C (62-24-14 At.%) (Figures 24 and 25).

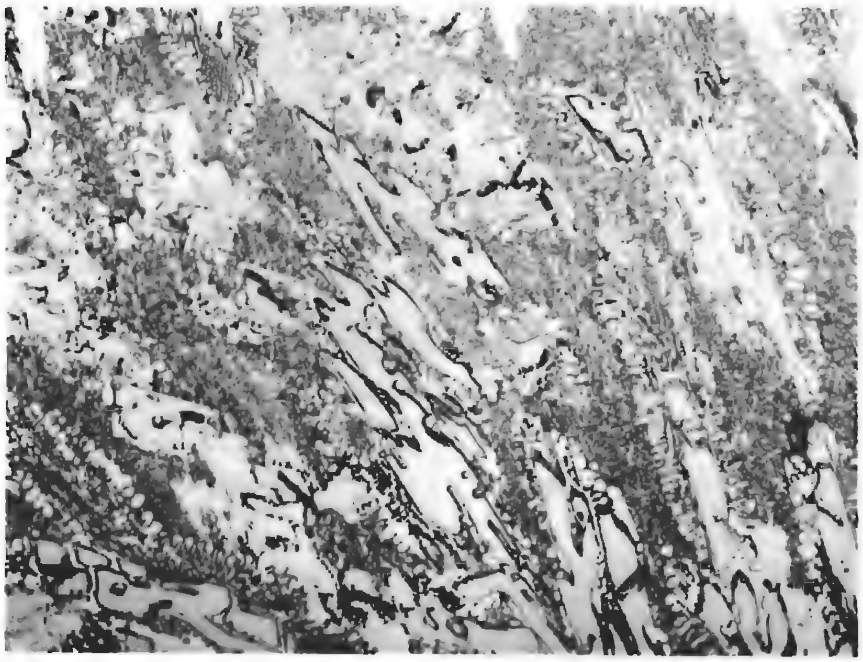

Figure 24. W-B-C (64-23-13 At.%), Rapidly Cooled from Liquidus Temperatures. X400

Small Amounts of Primary W_2B, Secondary W_2B and W_2C formed by Cocrystallization Along the Boundary Line $W_2B + W_2C$, and Ternary Eutectic $W_2B + W_2C + WB$.

A further ternary eutectic, at 2300° C and a composition W-B-C (55-26-19 At.%) consists of the phases $W_2C + WC + WB$ (Figures 26 and 27).

It is interesting to note, that the ternary range of existence of the cubic monocarbide α-WC_{1-x} is restricted to a very small concentration (< 3 At.% B) near the W-C binary, i.e. throughout its temperature range of existence, the α-WC_{1-x} phase does not form equilibria with any of the boride phases.

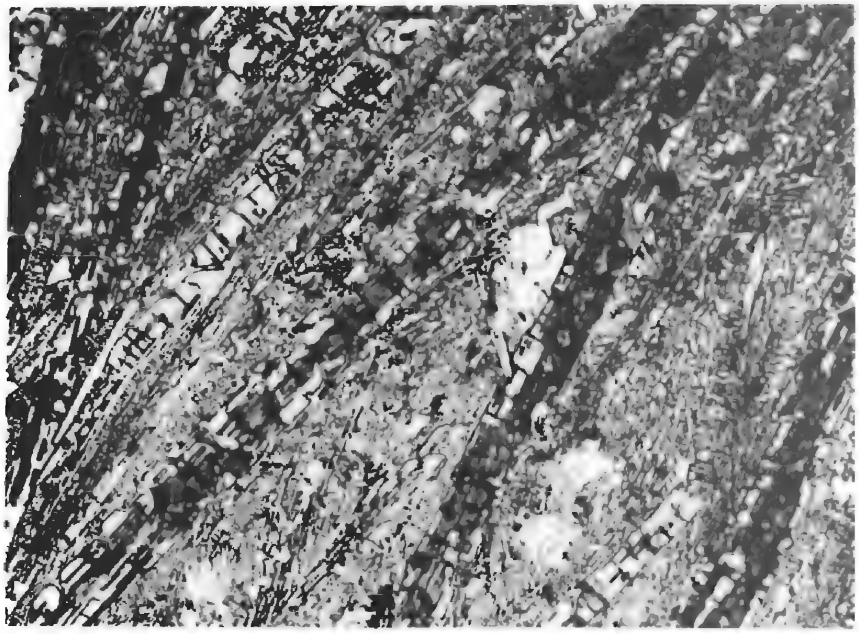

Figure 25. W-B-C (54-30-16 At.%), Rapidly Cooled from Liquidus Temperatures. X400

Elongated Crystals of Primary WB (Transformed) in a Ternary WB + W_2C + WC Eutectic Matrix.

Figure 26. W-B-C (55-25-20 At.%), Melted and Rapidly Cooled. X400

Trace of Primary W_2C in a Ternary W_2C + WC + WB Eutectic Structure.

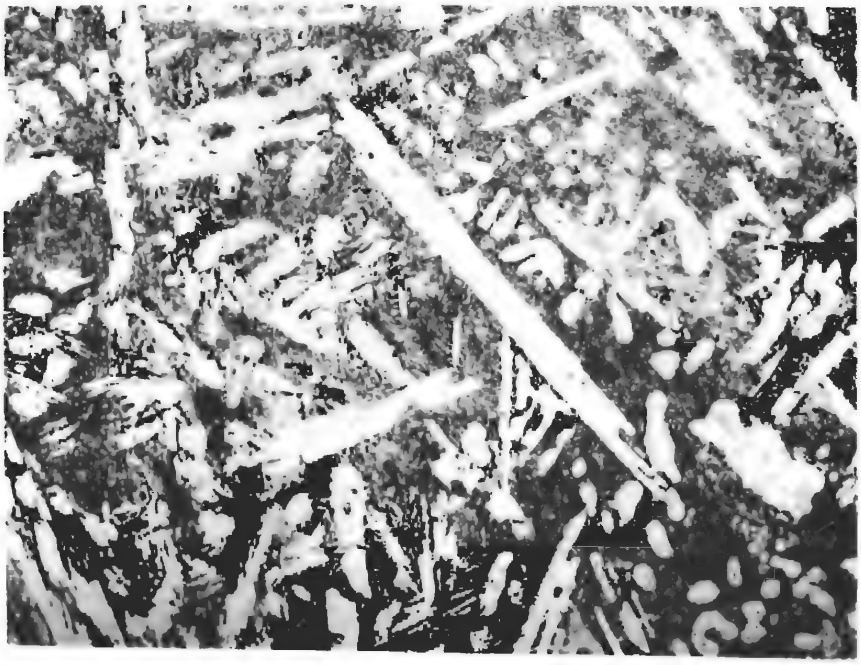

Figure 27. W-B-C (59-16-25 At.%), Melted and Rapidly Cooled. X400

Primary W_2C and W_2C + WC + WB Ternary Eutectic.

The investigation of the other sections of the system in the solidus range need not be described in detail, since the techniques were analogous to those described above, and the results, shown in data plots and a few selected micrographs in Figures 28 through 42, are selfexplanatory.

Figure 28. W-B-C (57-14-29 At.%), Rapidly Cooled from Liquidus Temperatures. X250

Primary WC, Bivariantly Crystallized W_2C + WC Eutectic-Like Structure, and Ternary W_2C + WC + WB Eutectic.

Note absence of free carbon, indicating that the sample is located between the boundary lines W_2C + WC and WC + C.

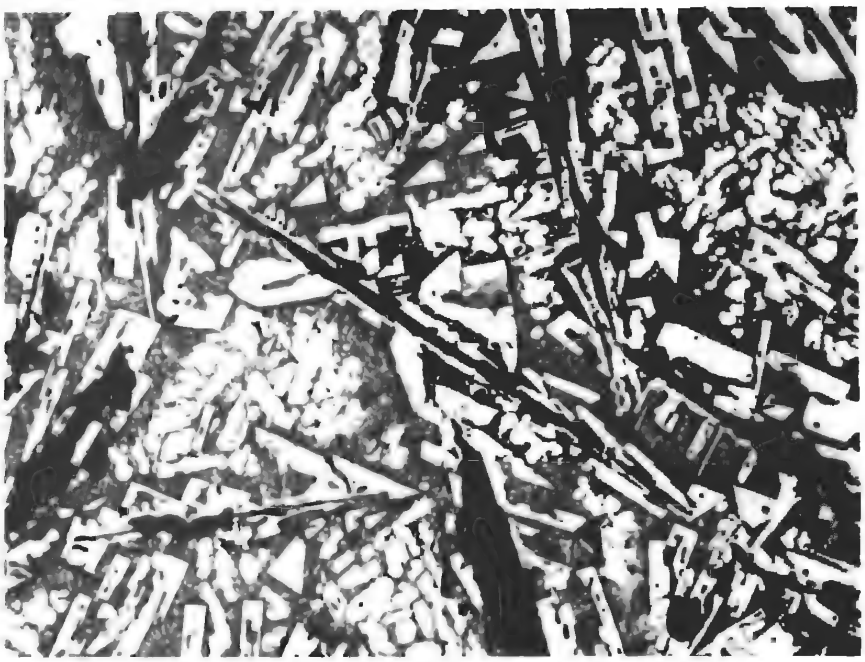

Figure 29. W-B-C (55-10-35 At.%), Rapidly Cooled from Liquidus Temperatures. X325

Primary Graphite Surrounded by Walls of Secondary WC, Traces of WB, and Ternary Eutectic W_2C + WC + WB.

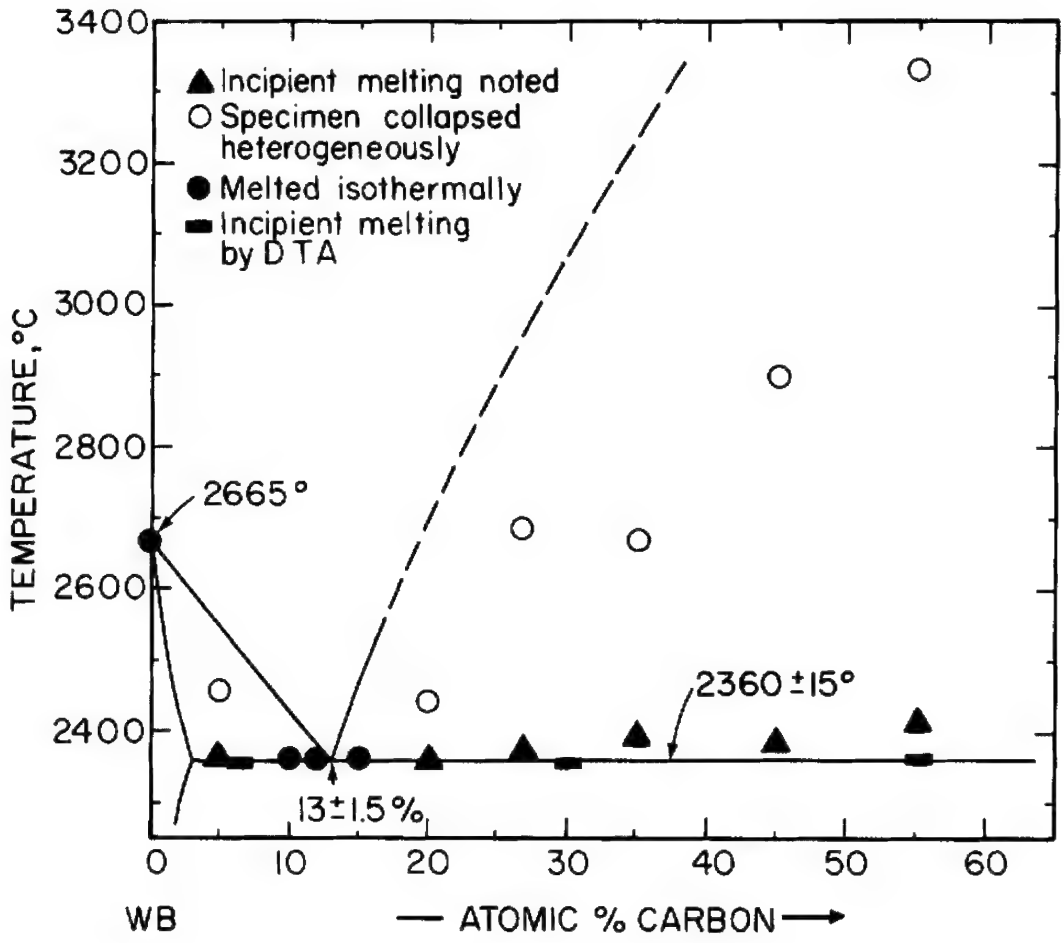

Figure 30. Experimental Melting Temperatures of Samples Located Along the Pseudobinary Section WB-C.

Figure 31. W-B-C (43-42-15 At.%), Melted and Rapidly Cooled. X475

Primary Graphite and Pseudobinary WB + C Eutectic.

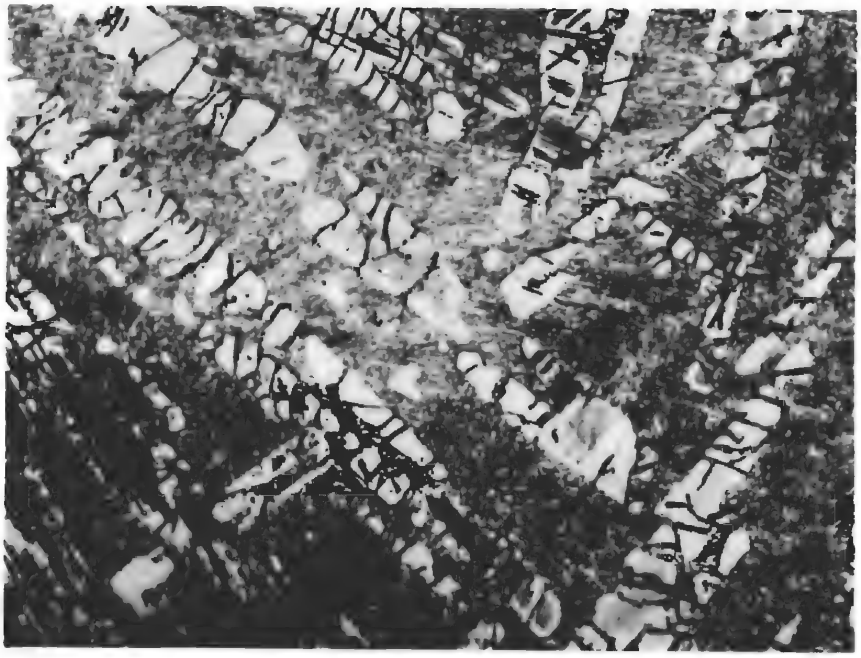

Figure 32. W-B-C (50-40-10 At.%), Melted and Rapidly Cooled. X400

Primary WB (Transformed) and Eutectic-Type Solidification Structure Formed Along the Boundary Line WC + WB and at the Ternary Eutectic W_2C + WC + W_2B Temperature.

Note absence of free carbon, indicating that the composition of the first product of crystallization lies below the WB + C boundary line.

Figure 33. W-B-C (45-35-20 At.%), Rapidly Cooled from Liquidus Temperatures. X525

Primary Graphite in a Eutectic-Like Solidification Structure Formed Along the Boundary Lines WB + C, WB + WC, and at the Ternary Eutectic Point WB + W_2C + WC.

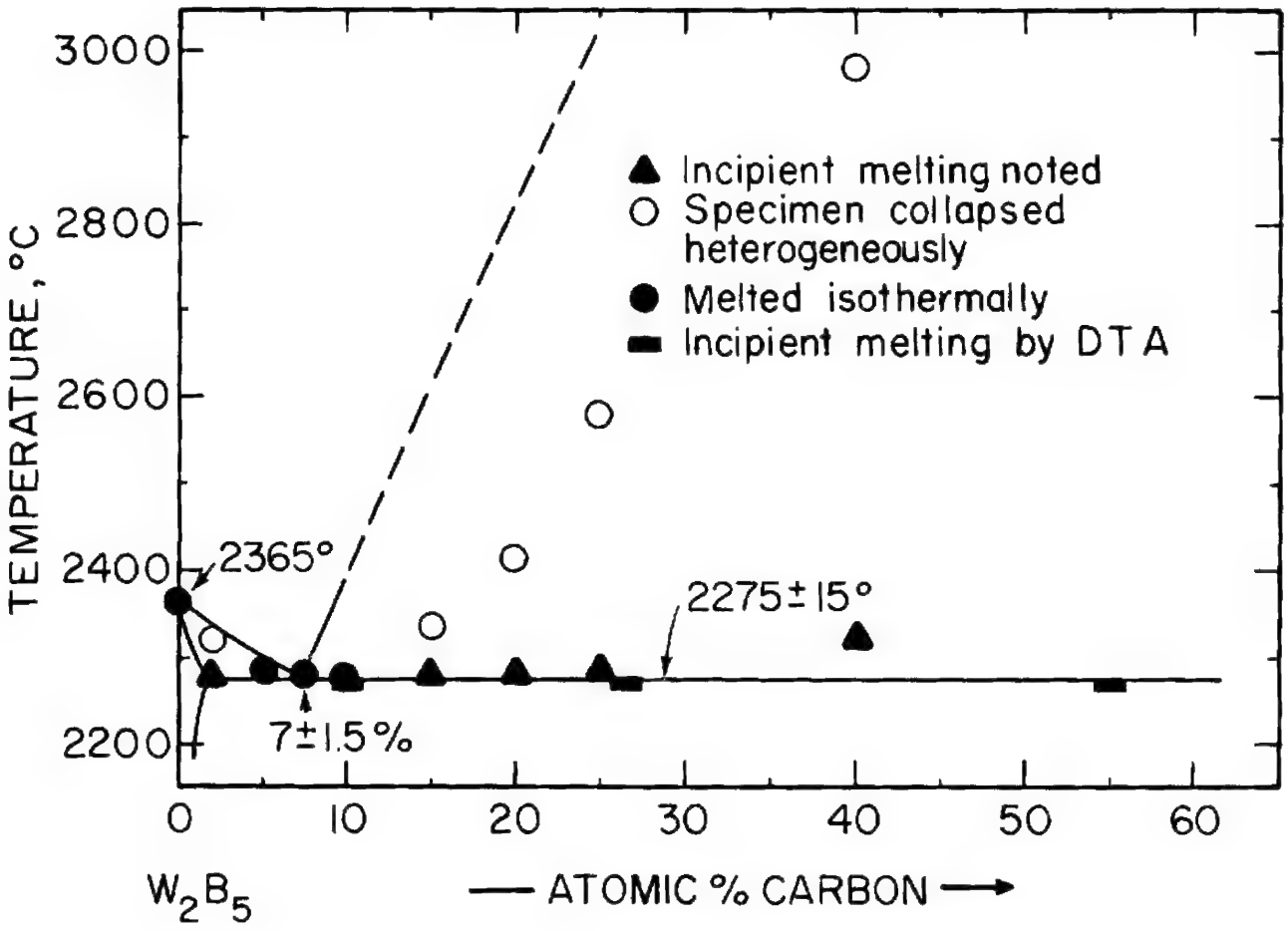

Figure 34. Melting Temperatures of Alloys Located Along the Pseudobinary Section W_2B_5-C.

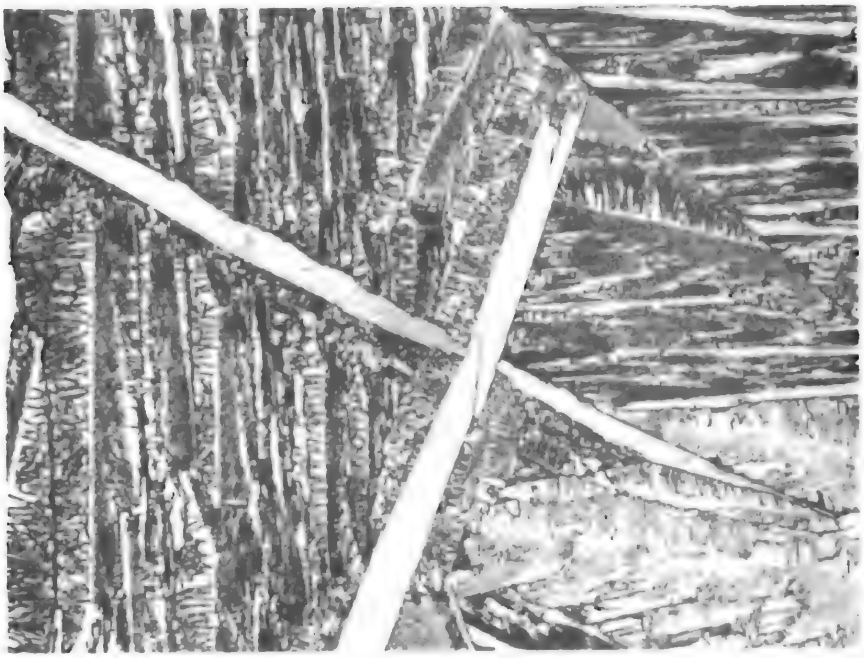

Figure 35. W-B-C (31-64-5 At.%), Rapidly Cooled from Liquidus Temperatures. X250

Primary W_2B_5 in a Pseudobinary W_2B_5 + C Eutectic Matrix.

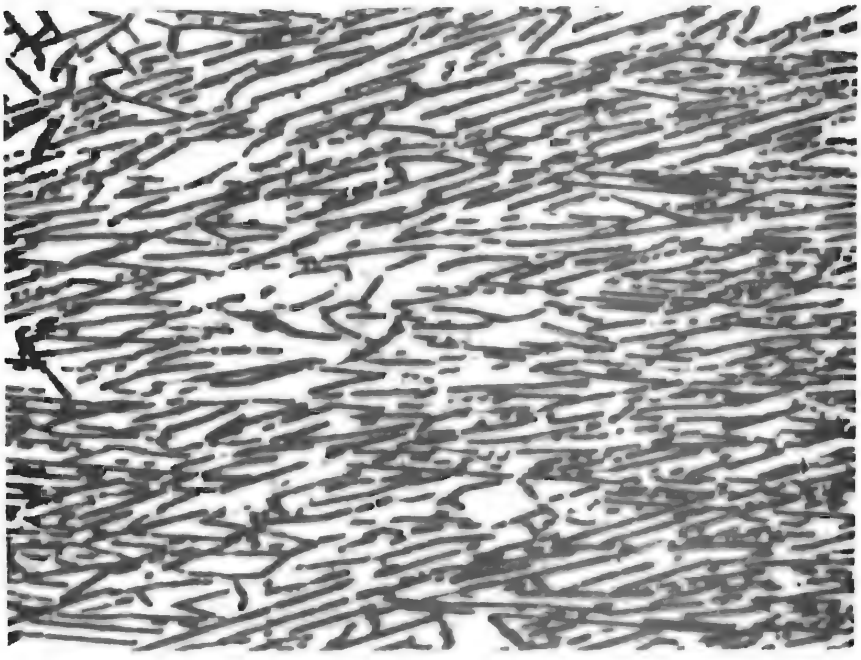

Figure 36. W-B-C (30-63-7 At.%), Rapidly Cooled from Liquidus Temperatures. X625

W_2B_5 + C Pseudobinary Eutectic.

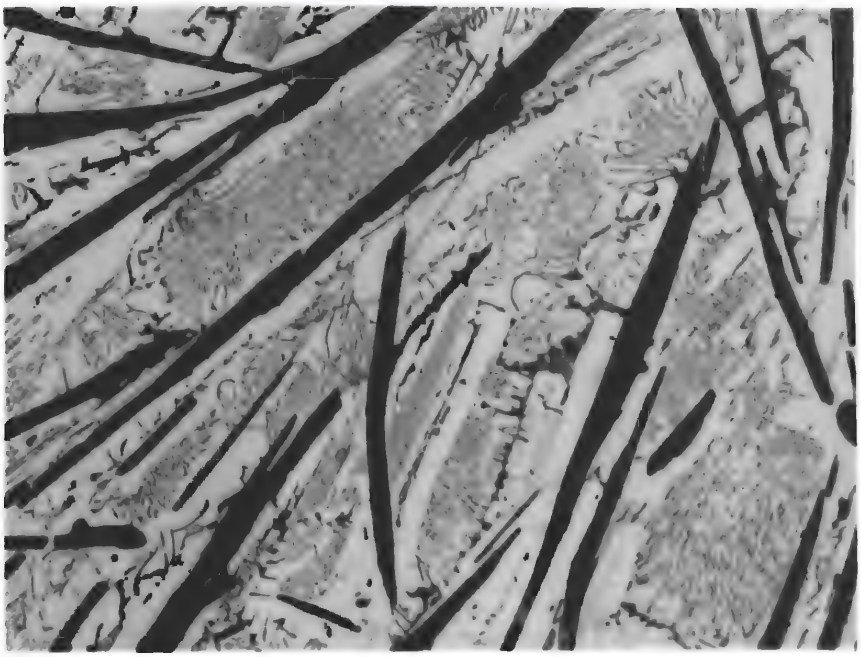

Figure 37. W-B-C (26-54-20 At.%), Melted and Rapidly Cooled. X350

Primary Graphite in a Partially Divorced, Pseudobinary W_2B_5 + C Eutectic Matrix.

Figure 38. W-B-C (39-56-5 At.%), Melted and Rapidly Cooled. X375.

Primary WB (Transformed), Secondary WB + C, and Ternary Eutectic WB + W_2B_5 + C.

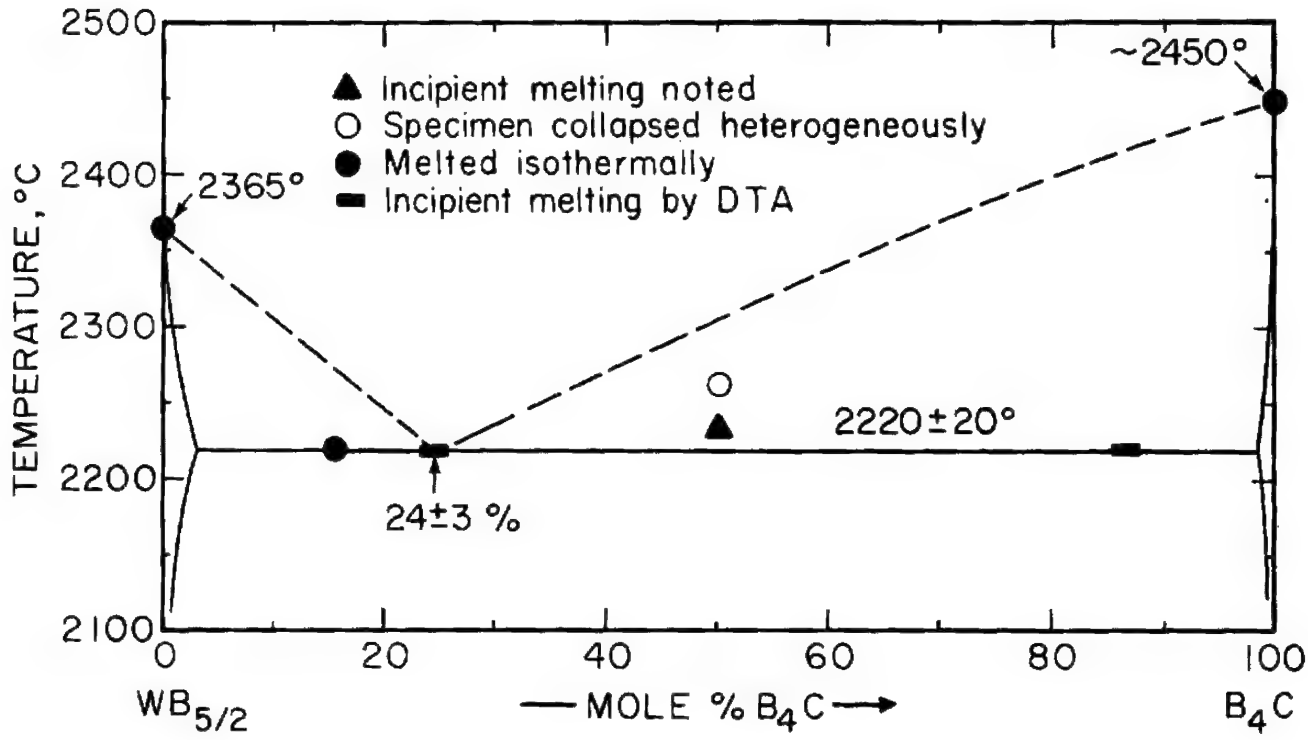

Figure 39. Melting Temperatures of Alloys Located at the Pseudobinary Section W_2B_5-B_4C.

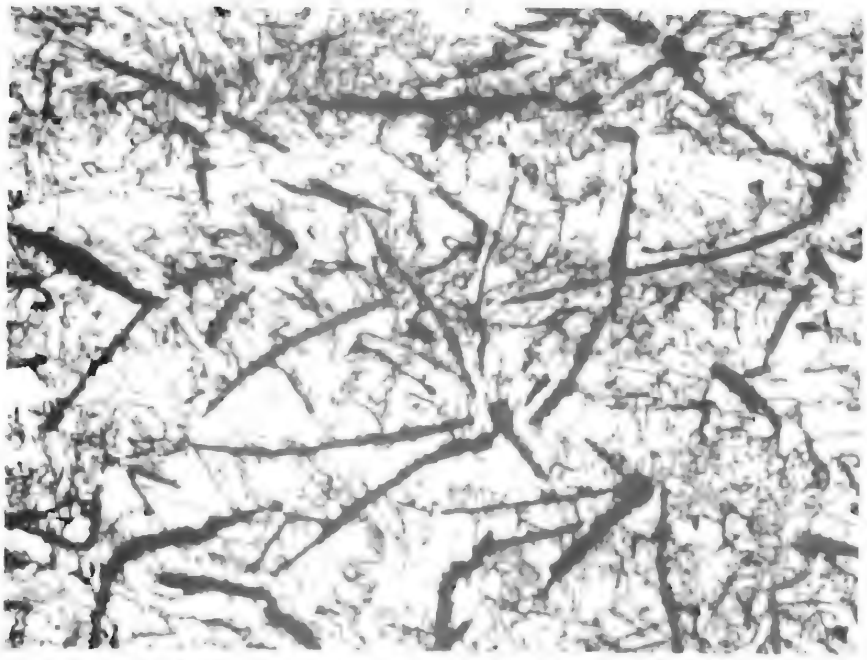

Figure 40. W-B-C (34-55-11 At.%), Melted and Rapidly Cooled. X475

Primary Graphite, Cocrystallized WB + C, and Ternary Eutectic WB + W_2B_5 + C.

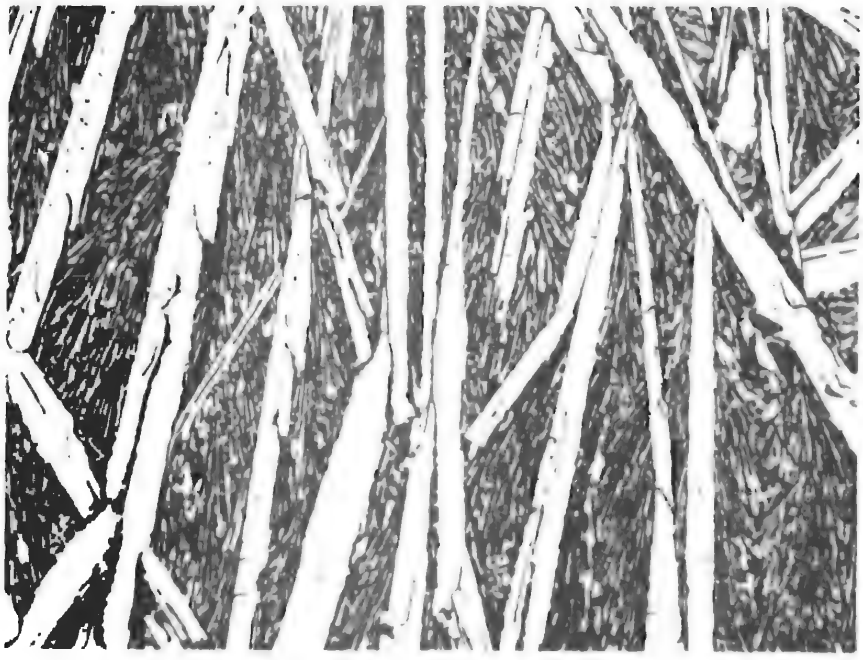

Figure 41. W-B-C (25-70-5 At.%), Melted and Rapidly Cooled. X275

Primary W_2B_5 in a Matrix of Pseudobinary W_2B_5 + B_4C Eutectic.

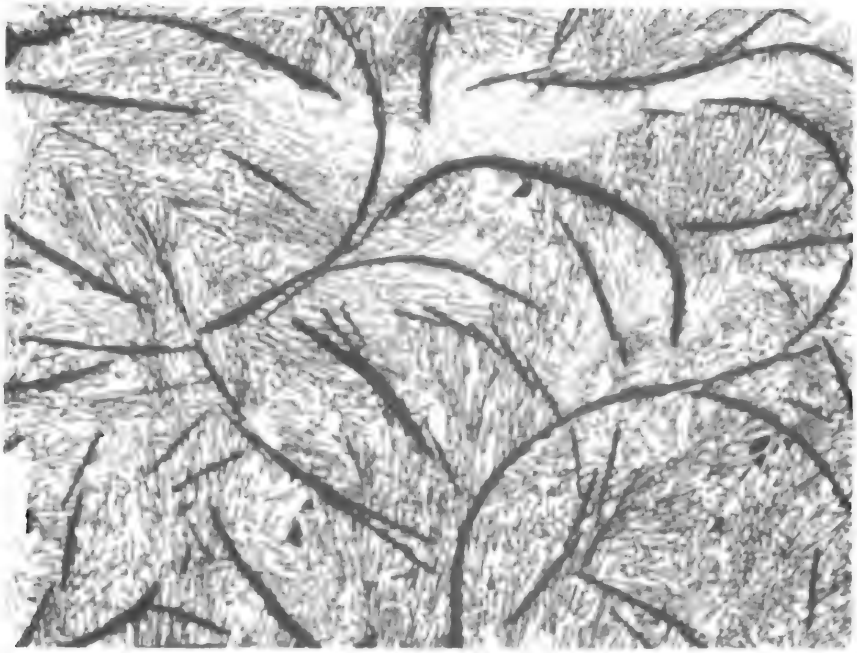

Figure 42. W-B-C (18-68-14 At.%), Melted and Rapidly Cooled. X270

Some Primary Graphite in an Alloy Located Close to the Ternary Eutectic $W_2B_5 + B_4C + C$. Also Note that the Ternary Eutectic Contains Only Small Amounts of Graphite.

B. ASSEMBLY OF THE PHASE DIAGRAM

The experimental results gathered in the course of the investigation have been combined to yield the phase diagram of the system shown in Figure 1. The diagram is supplemented by a flow diagram of isothermal binary and ternary reactions (Figure 2) and a projection of the liquidus surface, shown in Figure 3. For the convenience of use, and also to outline more clearly the temperature dependence of the phase equilibria in the system, a number of isothermal sections have been prepared and are shown in Figures 43 through 50.

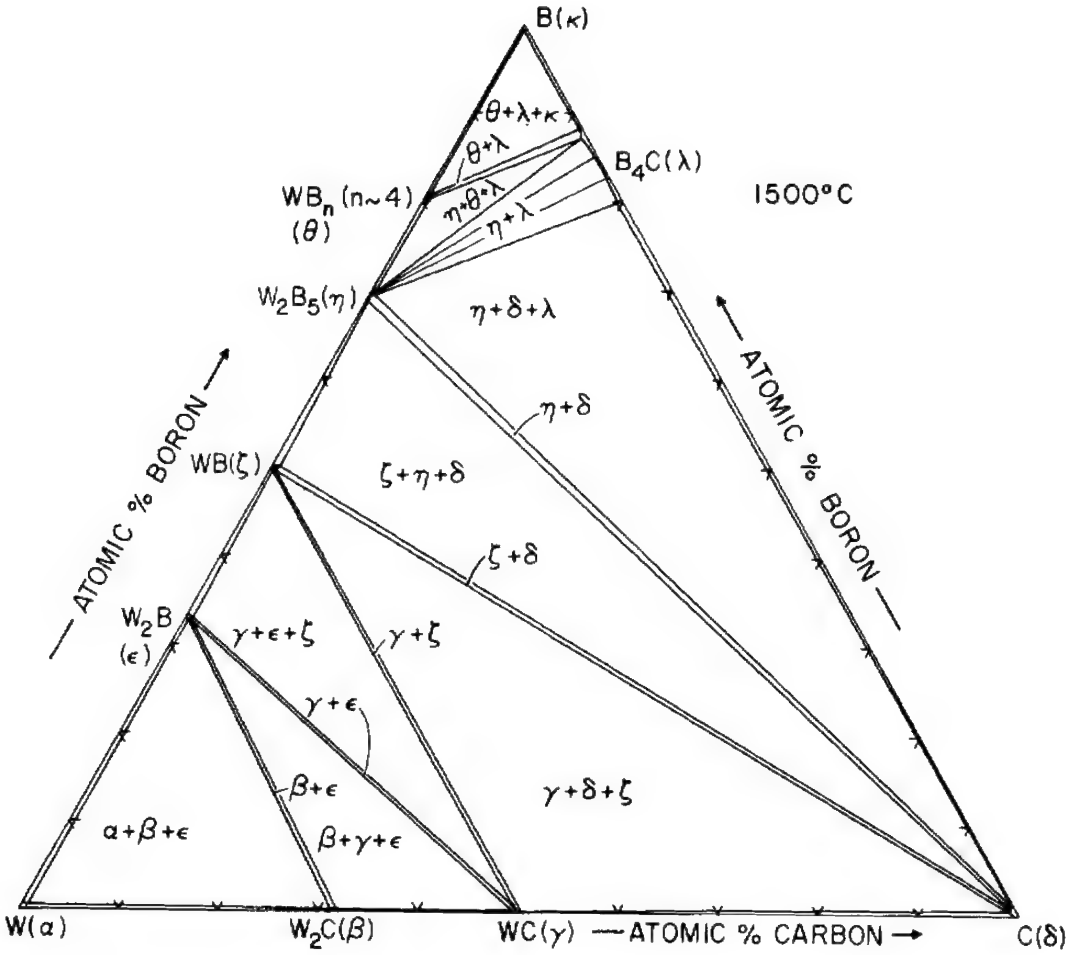

Figure 43. Isothermal Section of the W-B-C System at 1500° C.

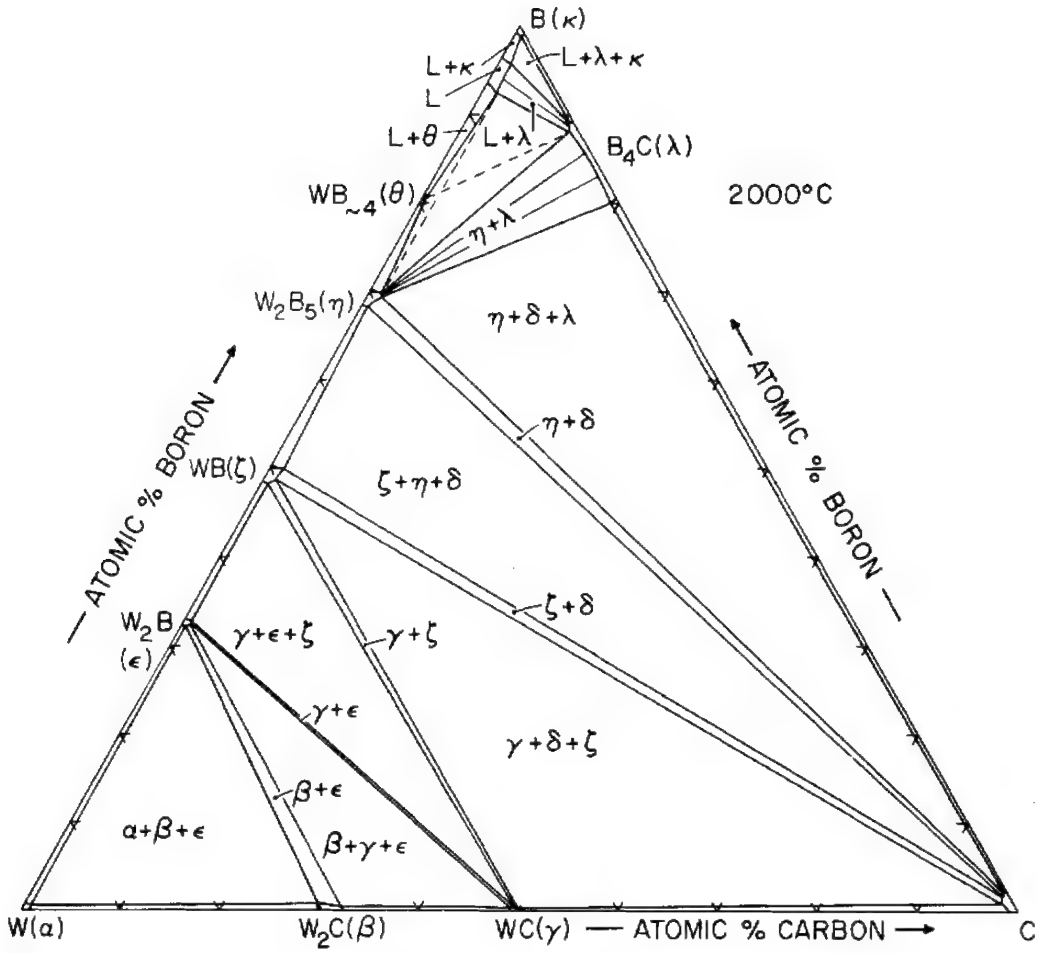

Figure 44. Isothermal Section of the W-B-C System at 2000° C.

Note 4-phase Plane (Class II Reaction)

$$L + B_4C \xrightarrow[T \leq 2000^\circ]{} WB_{\sim 4} + B_4C$$

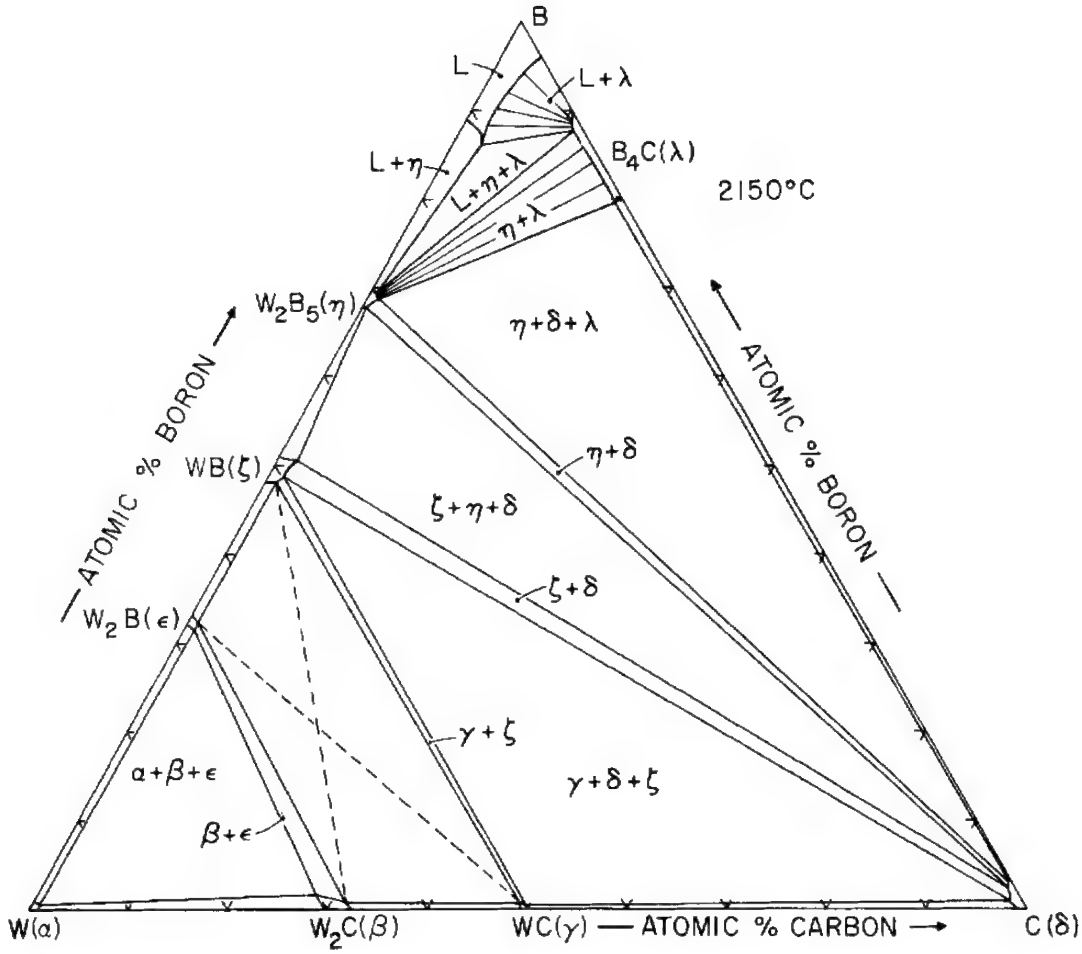

Figure 45. Isothermal Section of the W-B-C System at 2150°C.

Note 4-phase Plane (Class II Reaction)

$$WB + W_2C \xrightarrow[T \leq 2150^\circ]{} WC + W_2B$$

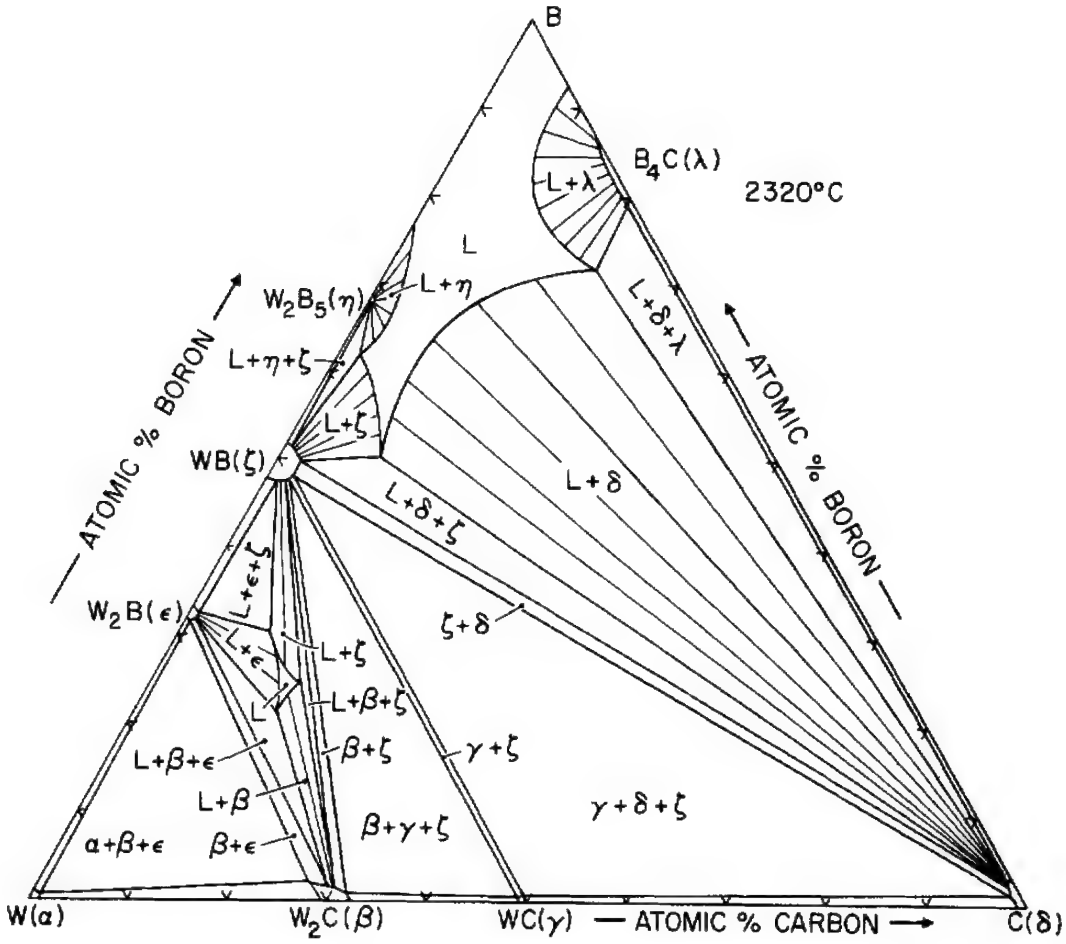

Figure 46. Isothermal Section of the W-B-C System at 2320° C.

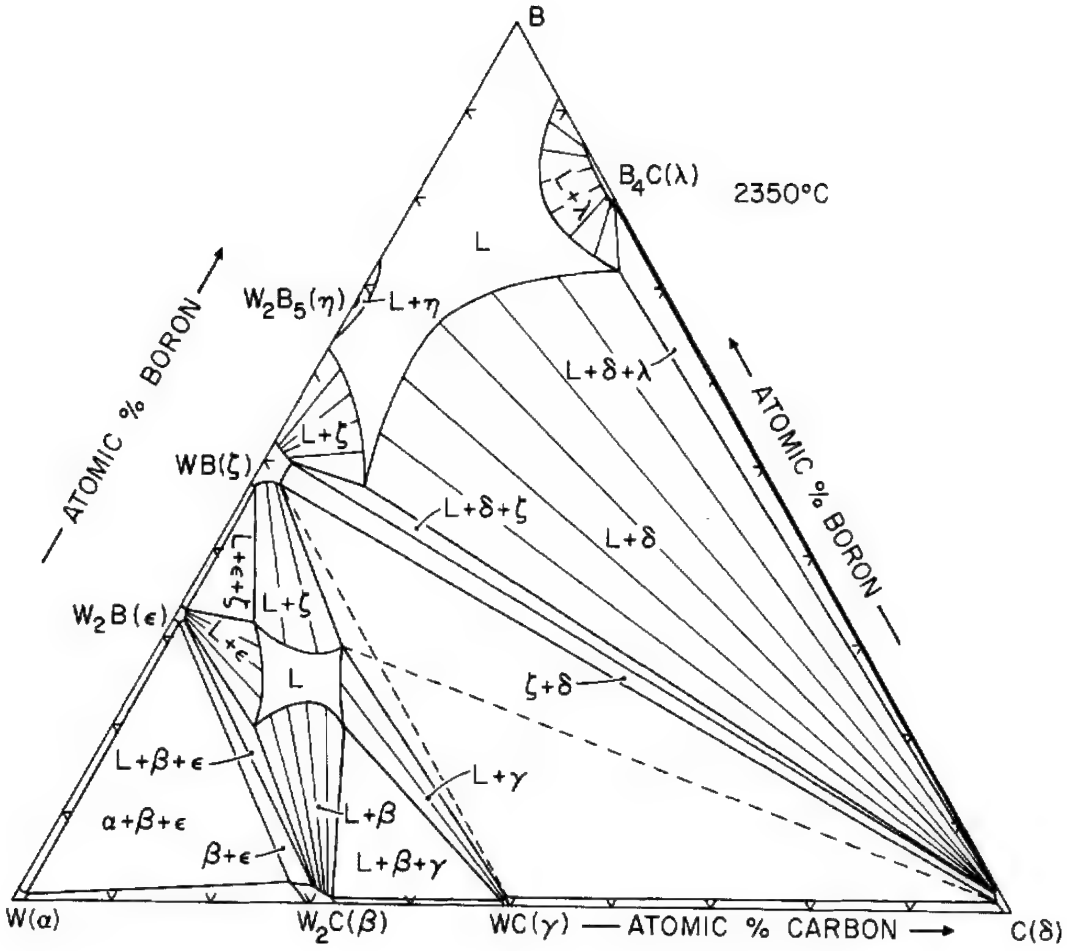

Figure 47. Isothermal Section of the W-B-C System at 2350°C.

Note 4-phase Plane (Class II Reaction)

$$L + C \xrightarrow[T \leq 2350^\circ]{} WB + WC$$

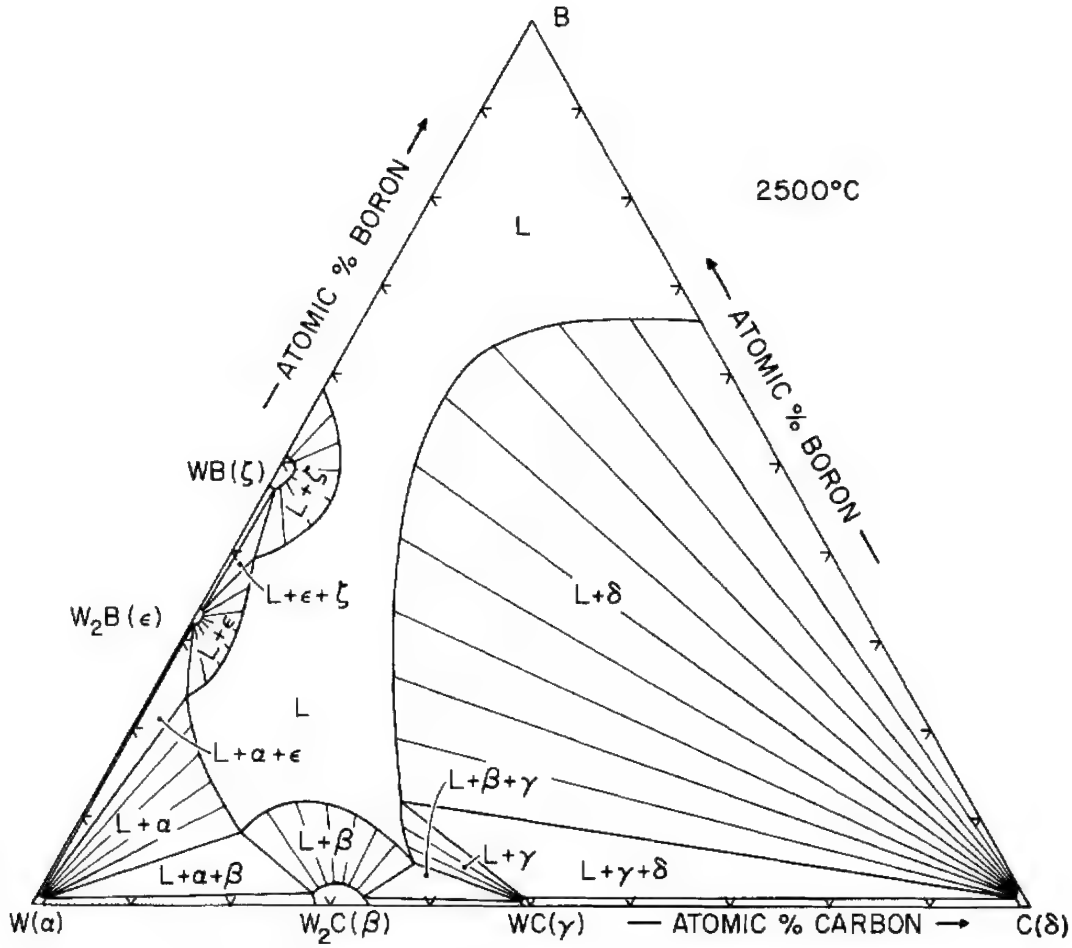

Figure 48. Isothermal Section of the W-B-C System at 2500° C.

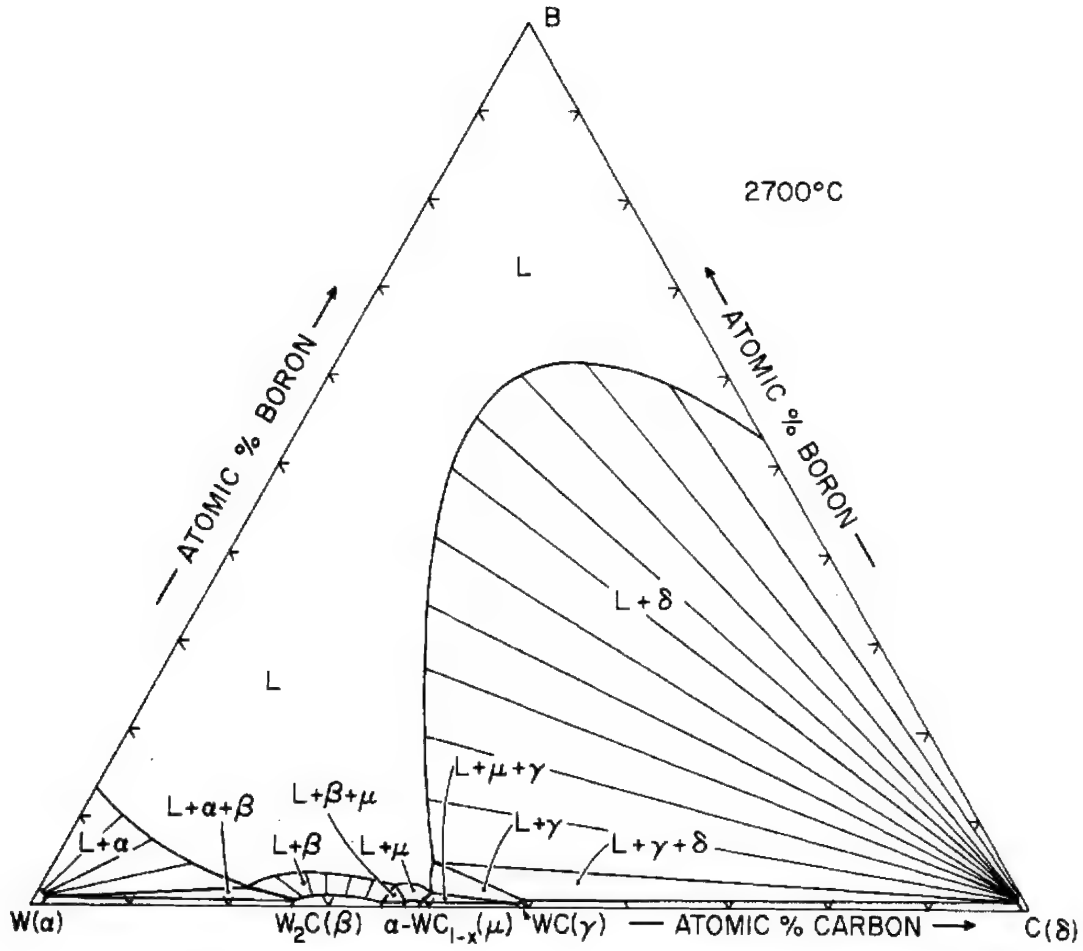

Figure 49. Isothermal Section of the W-B-C System at 2700°C.

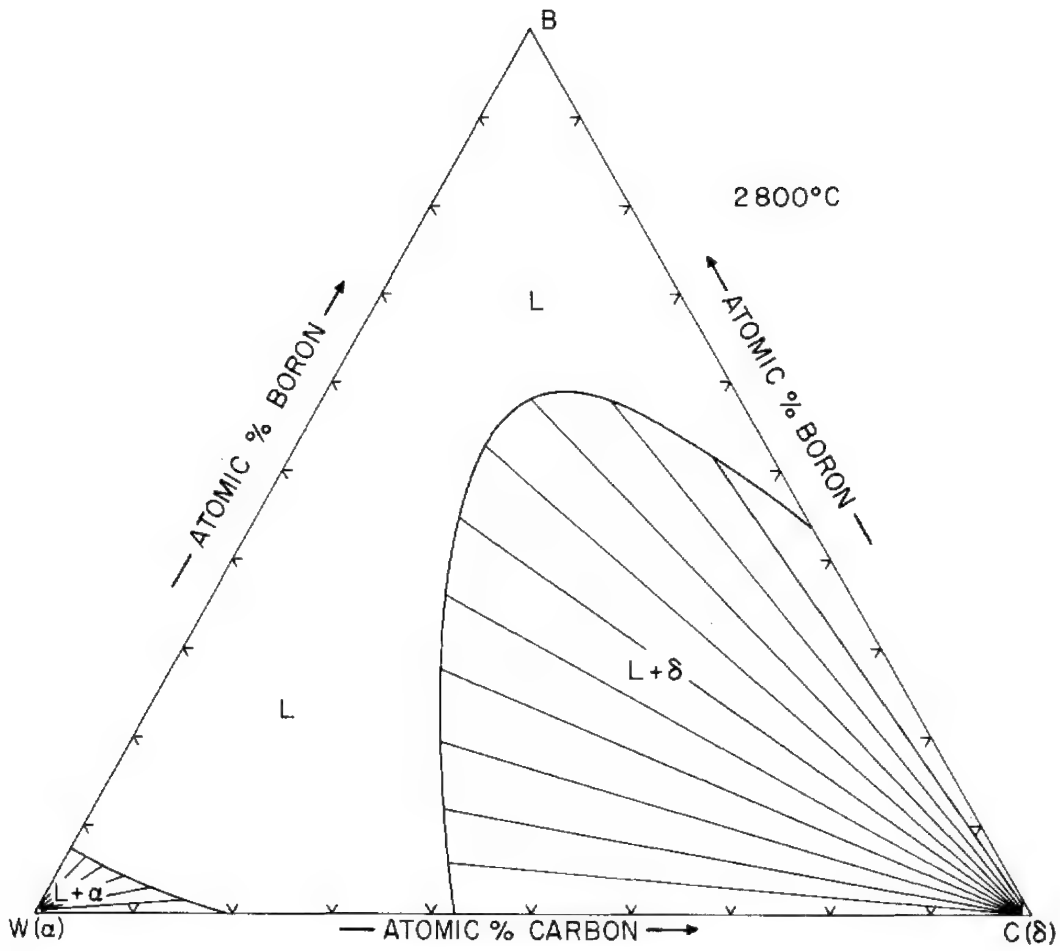

Figure 50. Isothermal Section of the W-B-C System at 2800°C.

V. DISCUSSION

The observed phase equilibria in the W-B-C system reflect the low stability of the carbides in relation to the borides, since the monoboride and W_2B_5 form stable equilibria with graphite. By comparison, in the boron-carbon systems of the group IV and group V metals[15,24], only the diborides form stable equilibria with graphite, besides being in equilibrium with the monocarbides.

The small mutual solubilities between carbides and borides, which is characteristic of all systems involving the refractory transition metals, is indicative of large stability differences between the respective crystal structures. As an example, the free energies of transformation of the stable modification of W_2B into the lattice type of W_2C and that of W_2C into the W_2B type, must be larger than 15 kcal/mole so as to account for the observed metal exchanges; the transformation energies for WB and WC are of the same order of magnitude.

Concerning the technical application of W-B-C alloys, several phase diagram features and observations made during the phase diagram study concerning alloy properties are of interest.

$B_4C + W_2B_5$ eutectic alloys show excellent castability and have surprisingly good mechanical impact resistance. Oxidation tests carried out at 1000° C showed good resistance to air attack, probably as a result of a highly viscous and tightly adhering film of boric acid at the surface of the specimens. Other alloys which could be of interest are the pseudobinary eutectics of the WB and W_2B_5 phases with graphite; the presence of the finely divided graphite in the eutectic provides a quasi-homogeneous structure with considerably lower bulk modulus, and thus better thermal shock sensitivity, than the pure binary phases. The applicability of other ternary W-B-C alloys,

notably the pseudobinary and ternary eutectics involving the W_2C, W_2B, WB, and WC phases, appears unlikely as a result of their extreme brittleness.

REFERENCES

1. U.S. Air Force Contract AF 33(615)-1249 (1964 to 1968), and U. S. Air Force Contract AF 33(615)-67-C-1513 (1967-1970). Report Series AFML-TR-65-2 and AFML-69-117, Air Force Materials Laboratory, Wright-Patterson Air Force Base, Ohio.

2. R. T. Doloff and R. V. Sara: WADD TR 60-143, Part II, Wright Air Development Division, Wright-Patterson Air Force Base, Ohio (1961).

3. R. V. Sara: J.Amer.Ceram.Soc., 48 (1965), 251.

4. E. K. Storms: The Refractory Carbides (Academic Press 1967).

5. E. Rudy, St. Windisch, and J. R. Hoffman: U.S. Air Force Tech. Rept. AFML-TR-65-2, Part I, Vol. VI (Jan 1966); AFML-TR-65-2, Part V (June 1969), Air Force Materials Laboratory, Wright-Patterson Air Force Base, Ohio.

6. E. Rudy and J. R. Hoffman: Planseeber. Pulvermet. 15 (1967), 174.

7. E. Rudy and St. Windisch: J.Amer.Ceramic Soc., 50 (1967), 272.

8. L.N. Butorina and Z.G. Pinsker: Kristallografiya, 5 (1960), 585.

9. K. Yvon, H. Nowotny, and F. Benesovsky: Monatsh. Chem., 99 (1968), 726.

10. W.B. Pearson: Handbook of Lattice Spacings and Structure of Metals and Alloys (Pergamon, 1958).

11. R. Kiessling: Acta. Chem. Scand. 1 (1947), 893.

12. E. Rudy and St. Windisch: U.S. Air Force Tech. Rept. AFML-TR-65-2, Part I, Vol. III, Air Force Materials Laboratory, Wright-Patterson Air Force Base, Ohio (July 1965).

13. B. Post and F. W. Glaser: J. Chem. Phys. 20 (1952), 1050.

14. P.A. Romans and M.P. King: Acta Cryst. 20 (1966), 313.

15. E. Rudy, F. Benesovsky, and L. Toth: Z. Metallkde, 54 (1063), 345.

References (Cont'd)

16. Compare the compilation of earlier data in R.P. Elliott: Constitution of Binary Alloys, First Supplement (McGraw-Hill, 1965).

17. H.K. Clark and J.L. Hoard: J.Amer.Chem.Soc., 65 (1943), 2115.

18. R.T. Doloff: U.S. Air Force Tech. Rept. WADD 60-143, Part I, Wright Air Development Division, Wright-Patterson Air Force Base, Ohio, (1960).

19. R. P. Elliott: U. S. AEC Contract AT (11-1)-578, Final Report ARF-2200-12 (1961).

20. F. W. Glaser: J. Metals, 4 (1952), 391.

21. L. Brewer and H. Haraldsen: J. Electrochem.Soc., 102 (1953), 399.

22. E. Rudy and G. Progulski: Planseeber.Pulvermet., 15 (1967), 13. U.S. Air Force Tech. Report, AFML-TR-65-2, Part III, Vol. II, Air Force Materials Laboratory, Wright-Patterson Air Force Base, Ohio, (April 1966).

Unclassified
Security Classification

DOCUMENT CONTROL DATA - R & D

(Security classification of title, body of abstract and indexing annotation must be entered when the overall report is classified)

1. ORIGINATING ACTIVITY (Corporate author)
Materials Research Laboratory
Aerojet-General Corporation
Sacramento, California

2a. REPORT SECURITY CLASSIFICATION
Unclassified

2b. GROUP
N.A.

3. REPORT TITLE
Experimental Phase Equilibria of Selected Binary, Ternary, and Higher Order Systems.
Part V, The Phase Diagram W-B-C

4. DESCRIPTIVE NOTES (Type of report and inclusive dates)
April 1967 - May 1969

5. AUTHOR(S) (First name, middle initial, last name)
Rudy, E.

6. REPORT DATE	7a. TOTAL NO. OF PAGES	7b. NO. OF REFS
August 1970	51	24

8a. CONTRACT OR GRANT NO.	9a. ORIGINATOR'S REPORT NUMBER(S)
F 33 615-67-C-1513	
b. PROJECT NO. 7350	
c. Task No. 735001	9b. OTHER REPORT NO(S) (Any other numbers that may be assigned this report)
d.	AFML-TR-69-117 Part V

10. DISTRIBUTION STATEMENT
This document has been approved for public release and sale; its distribution is unlimited.

11. SUPPLEMENTARY NOTES	12. SPONSORING MILITARY ACTIVITY
	Air Force Materials Laboratory (MAMC) Wright-Patterson AFB, Ohio 45433

13. ABSTRACT

The ternary alloy system W-B-C was investigated experimentally by means of X-ray, melting point, DTA, and metallographic techniques on hot pressed and heat treated, as well as melted specimens, and a phase diagram from 1500° C through the melting range established.

No ternary phases are formed in the system and the mutual solubilities between carbide and boride phases are small. The solid state sections (<2000° C) are characterized by two-phase equilibria existing between the phase pairs $W_2B + W_2C$, $W_2B + WC$, $WC + WB$, $WB + C$, $W_2B_5 + C$, $W_2B_5 + B_4C$, and $WB_{\sim 4} + B_4C$. The two-phase equilibrium $W_2B + WC$ is replaced by an equilibrium $W_2C + WB$ above 2150° C.

Fifteen ternary isothermal reactions have been found. Five are associated with pseudobinary eutectic equilibria, six with ternary eutectics, and the remaining four with class II ternary four-phase reaction isotherms.

DD FORM 1 NOV 65 1473

Unclassified
Security Classification

Unclassified
Security Classification

14. KEY WORDS	LINK A		LINK B		LINK C	
	ROLE	WT	ROLE	WT	ROLE	WT
Refractory Carbides Phase Equilibria W-B-C						

Unclassified
Security Classification